

# The Mission Defines the Cycle: Turbojet, Turbofan and Variable Cycle Engines for High Speed Propulsion

**Joachim Kurzke**  
Max Feldbauer Weg 5  
85221 Dachau  
GERMANY

[kurzke@gasturb.de](mailto:kurzke@gasturb.de)

## SUMMARY

*High speed propulsion employing turbojets, turbofans and variable cycle engines is interpreted here as propulsion for supersonic air vehicles with flight Mach numbers up to the technical limits of the gas turbine. This limit is somewhere between flight Mach numbers of 3 to 4. If the mission asks for higher vehicle speeds then other propulsion concepts need to be considered, eventually in combination with gas turbines dedicated to take off, acceleration and the return segments of the mission.*

*First the thermodynamic cycles of dry and reheated turbojets as well as turbofans are examined at supersonic flight Mach numbers. All point performance calculations are done for altitude/Mach number combinations on a line in the middle of a typical flight envelope with constant equivalent airspeed EAS. For the flight condition of Mach 2 at 11km altitude it is shown that for a given thrust the size of a dry turbofan is significantly bigger than that of an engine with afterburner.*

*However, all the engines must not only be able to operate at their supersonic design condition but also at all the combinations of Mach number and altitude on the flight path from take off to maximum speed. This off-design requirement influences the selection of the aerodynamic compressor design point and consequently also the size of the turbomachines.*

*A short section about variable cycle engines explains with an example how such a machine operates with the various settings of flow diverter valves, mixer and nozzle area. It is shown that in addition to these adjustable geometry elements the core driven fan stage needs variable inlet guide vanes.*

*Finally two components that are not found in engines designed for subsonic flight are described in some detail with examples: the afterburner and the variable area convergent divergent nozzle.*

## 1.0 INTRODUCTION

Whatever the propulsion concept is, the flight envelope of any vehicle to be launched from an airfield begins at the lower end with sea level static. Take off is an important off-design condition for a gas turbine designed for supersonic propulsion. The flight envelope is limited by two boundaries that are approximately lines of constant equivalent air speed EAS. The lower EAS boundary represents an aerodynamic limit of the aircraft (maximum lift coefficient), the upper boundary is a structural limit of the air vehicle.

Figure 1 shows a flight envelope with 200 and 700knots as boundaries together with lines of constant stagnation temperature. The EAS boundary values are typical for modern fighter aircraft with a maximum speed of around Mach 2. Air vehicles designed for Mach 3+ have a much more narrow flight envelope with boundaries of 310 and 420knots in the case of the famous Blackbird SR-71, for example.

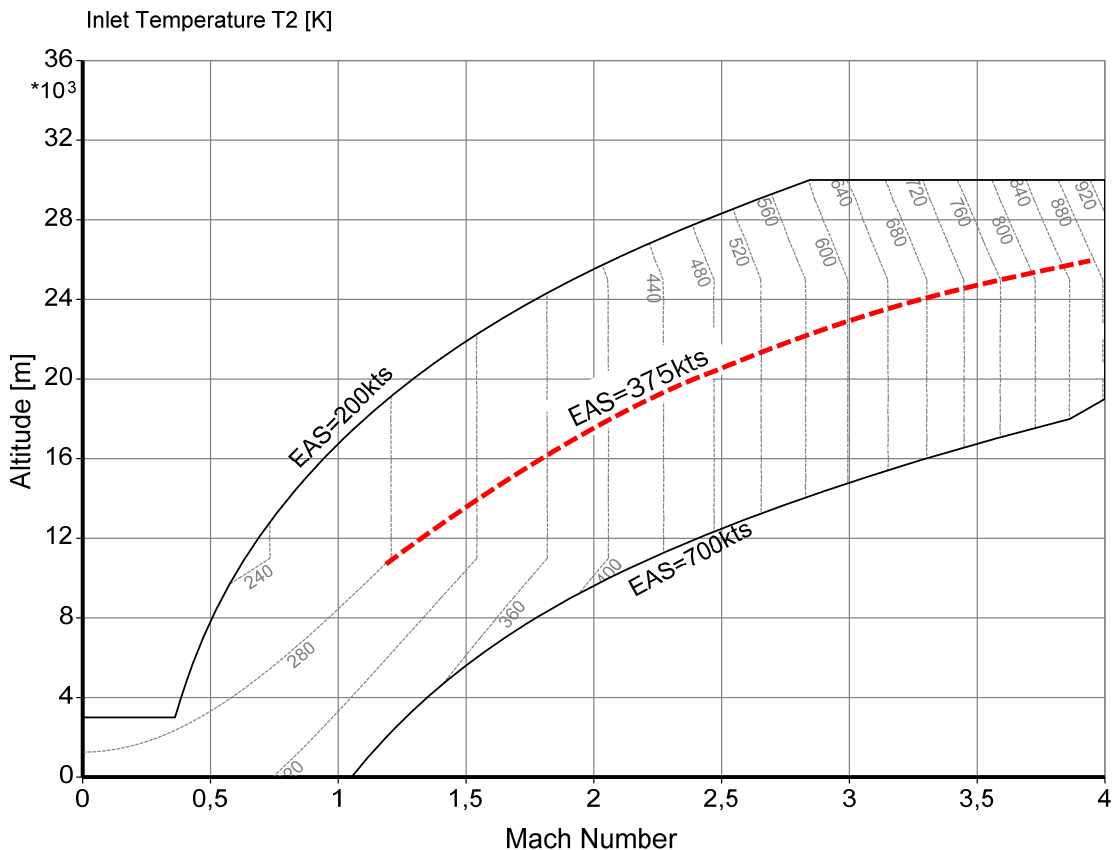


Figure 1: Flight Envelope.

From the figure one can read that the stagnation temperature at a Mach number of 4 is 890K. This value is near to the material temperature limit of modern compressor disks. There is only a small temperature margin left for compressing air – if that makes sense at all.

In the following we look at first at the thermodynamic cycle of engines that are designed to operate only at a single point in the flight envelope. The fact that any engine must operate satisfactorily also at take off will be considered later.

## 2.0 POINT PERFORMANCE

For evaluating the performance potential of various gas turbines it is convenient considering at first the thermodynamic cycle at selected flight conditions. For that purpose several points along a flight path in the middle of the SR-71 flight envelope (constant EAS=375knots) are selected for thermodynamic studies yielding numbers for specific fuel consumption and specific thrust (thrust per unit of airflow). Maximizing specific thrust means that for a given thrust requirement the engine has the smallest size.

All engines examined have polytropic efficiencies of 0.9 for both the compressors and turbines. With a burner exit temperature of 1500K for the cooling of the turbine inlet guide vane 2% of the compressor air flow air is used and for cooling the following turbine parts 1%. With  $T_4=2000K$  the amounts of cooling air are 10% and 6% respectively. Burner pressure ratio is taken into account with 0.97 and turbine exit duct pressure ratio is 0.98. Altogether these assumptions describe the state of the art of gas turbine design.

Inlet pressure recovery depends on Mach number as described by MIL-E-5007:

$$\frac{P_2}{P_1} = 1 - 0.075 * (Mn - 1)^{1.88}$$

The nozzle is modeled as an ideal convergent-divergent design - the exit area is such that the exhaust gases expand to ambient pressure.

## 2.1 Turbojet

### 2.1.1 “Dry” Turbojet

The most simple gas turbine is the straight turbojet as sketched in the top part of Figure 2. Figure 3 shows specific thrust (i.e. thrust per unit of air flow) and specific fuel consumption SFC for three altitude / Mach number conditions along the 375knots flight path. The highest burner exit temperature yields always the highest specific thrust. For the two lower Mach numbers of 1.2 and 1.8 a compressor pressure ratio of more than 30 yields the lowest specific fuel consumption. At the flight Mach number of 2.4 there is a SFC optimum with respect to pressure ratio around 20 to 22.5.

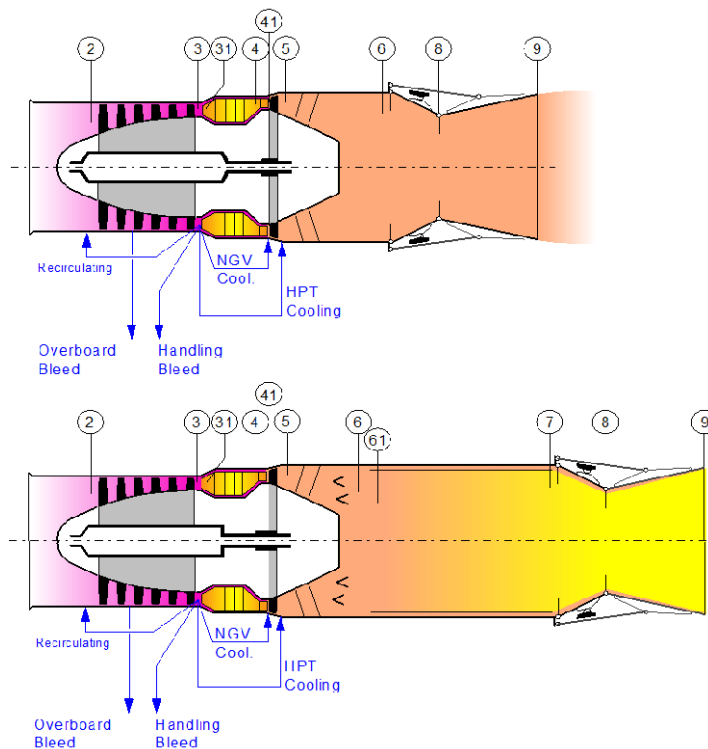


Figure 2: Turbojet Nomenclature.

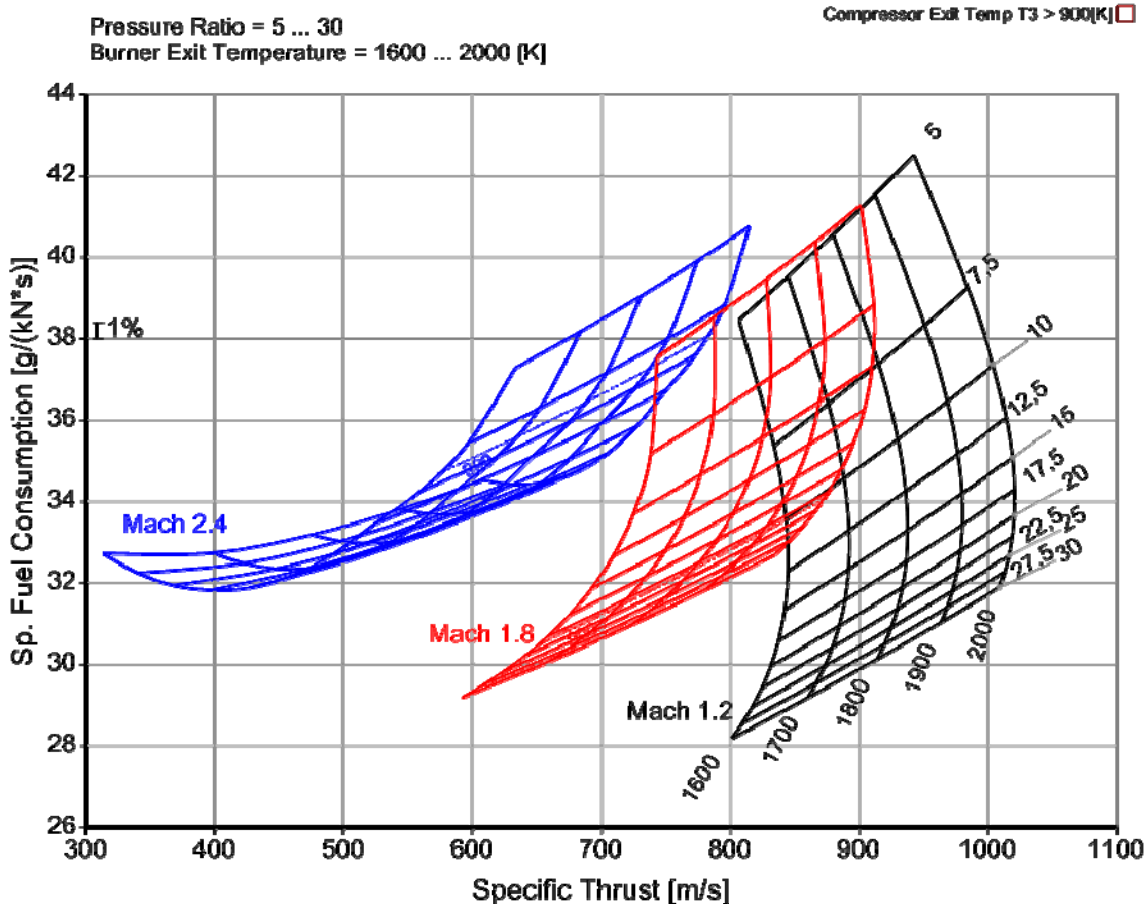


Figure 3: Dry Turbojet.

However, the thermodynamically optimal pressure ratio cannot be achieved in a real world application because the compressor exit temperature is limited to values not much higher than 900K. This limitation originates from the maximum tolerable compressor disk material temperature. Cooling the last compressor disk requires air that has sufficient pressure and this high pressure air has – if not cooled by some special means – the compressor delivery temperature. Therefore the pressure ratio is restricted at Mach 1.8 to around 21 and at Mach 2.4 to a value as low as 9, indicated by the dashed line in the respective carpet.

For the next examination, which covers the complete Mach number range along the flight path with 375knots, we select as burner exit temperature  $T_4=1900K$  and adjust the pressure ratio in such a way that the compressor delivery temperature is  $T_3=900K$ . Figure 4 shows four important parameters along the flight path. With the chosen assumptions the highest achievable Mach number is slightly below 4.

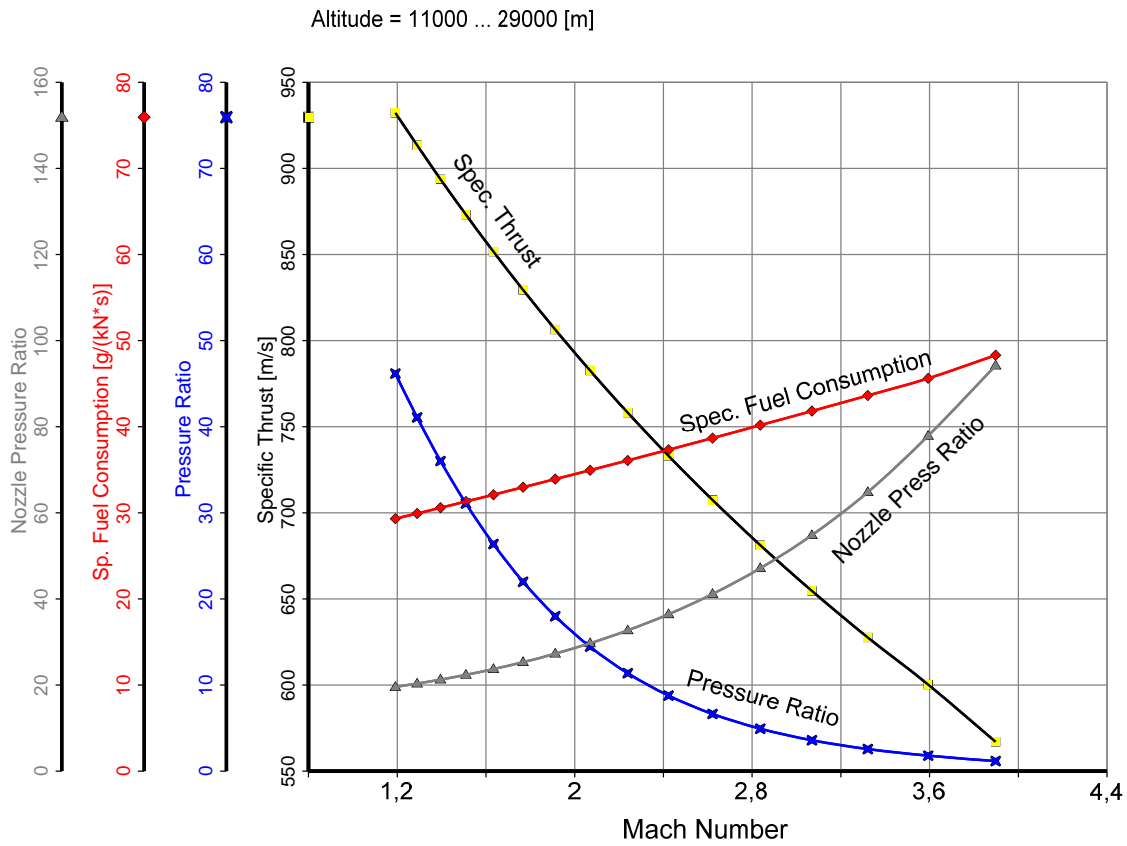


Figure 4: Dry Turbojet,  $T_3=900K$ .

Specific thrust decreases from 932 to 567m/s (-39%) which goes along with an increase of specific fuel consumption by +67% from 29.3 to 49 g/(kN\*s). Above Mach 3 the pressure ratio decreases from 4 to a value of little more than 1 at the top Mach number end. Obviously it does not make very much sense to employ a dry turbojet as the sole propulsor if the design Mach number is much higher than 3.

Note that in spite of the decreasing compressor pressure ratio the nozzle pressure ratio increases up to nearly 100 at the right end of the examined range of Mach numbers. There the nozzle inlet pressure is created nearly exclusively by the engine intake. Thus the quality of the propulsion system at very high flight speed is dominated by the intake and the nozzle performance. Compressor and turbine efficiencies are no longer important in such an application. The two temperature-entropy diagrams for Mach number 1.2 and 3.9 shown in Figure 5 make that obvious.

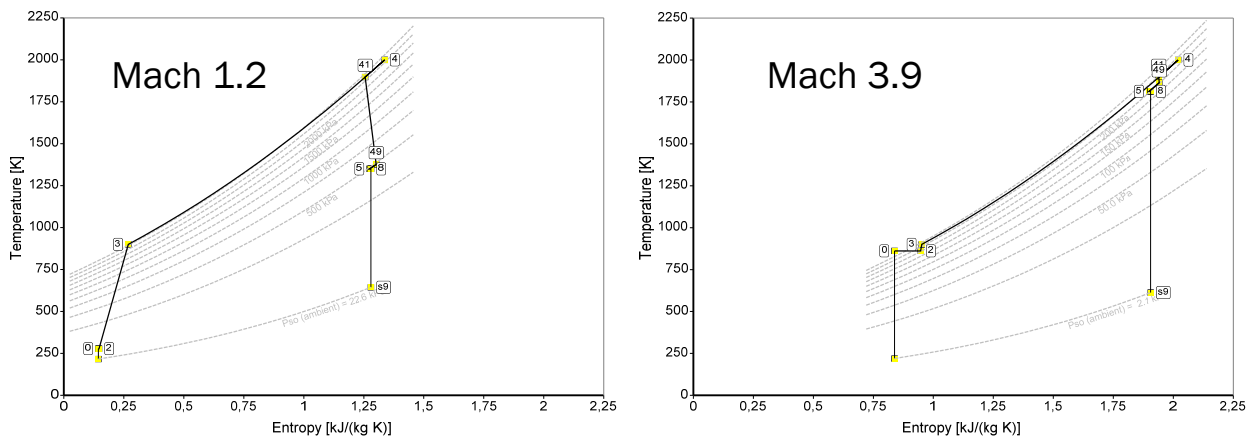


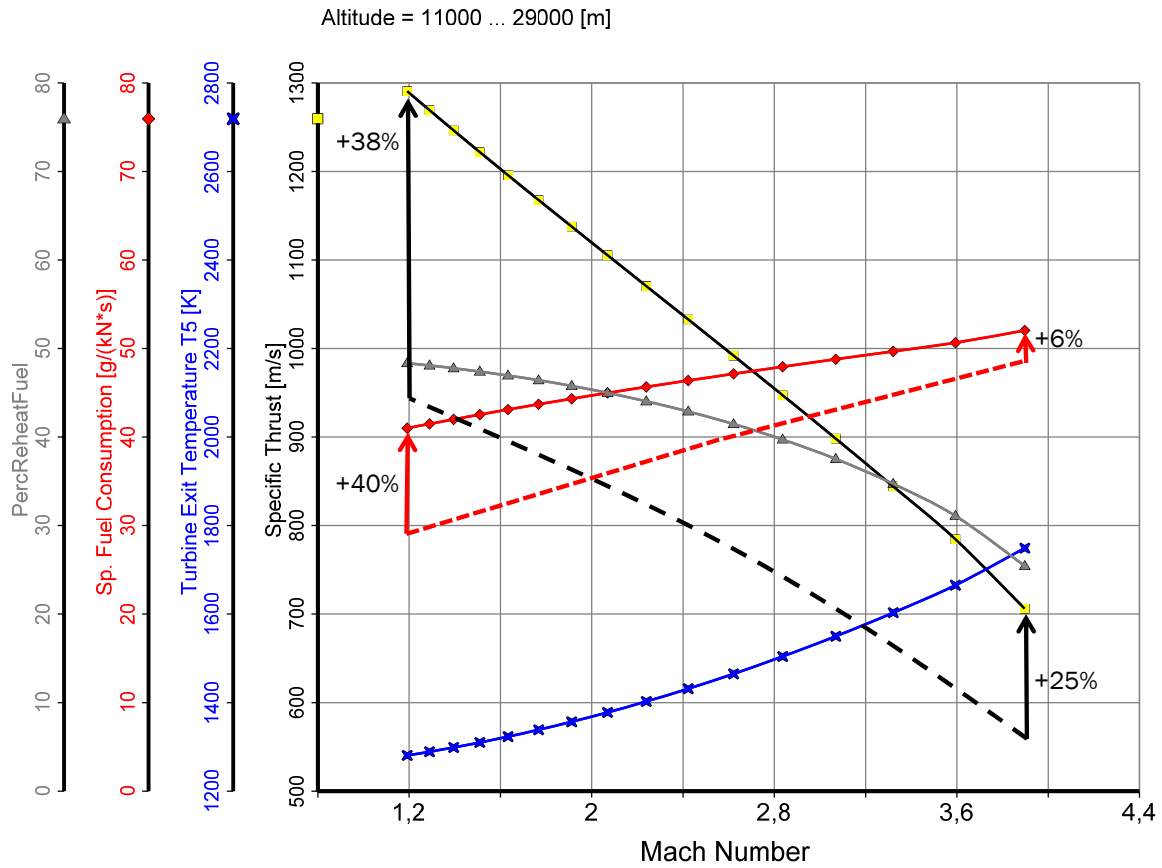
Figure 5: Dry Turbojet.

### 2.1.2 Turbojet with Reheat (Afterburner)

Thrust of a straight turbojet can be increased by adding a reheat system (an afterburner) which makes use of the remaining oxygen and increases the gas temperature from  $T_5$  (turbine exit temperature) to the reheat exit temperature  $T_7$  of about 2000K. This requires additional fuel and makes the “dry” turbojet to a “wet” turbojet.

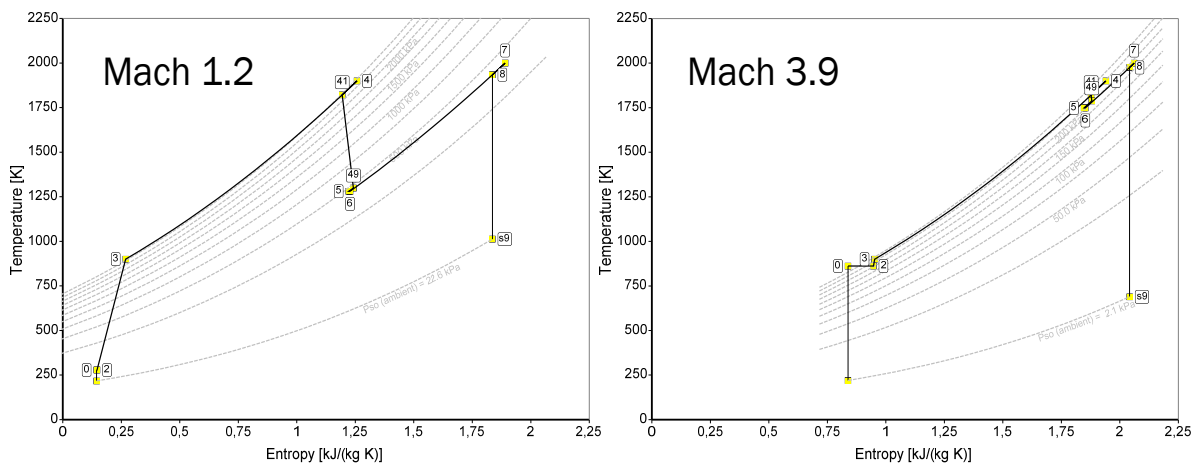
Due to the high gas velocity in the reheat pipe the burning efficiency is significantly less than in the main burner; the following cycle calculations employ a value of 90%. Cooling of the afterburner casing and the nozzle requires about 10% of the total mass flow. In the simulation the cooling air is mixed with the hot gases upstream of the nozzle throat.

Figure 6 compares specific thrust and specific fuel consumption of the dry turbojet with the wet (reheated) version. At the low Mach number end ( $M_n=1.2$ ) one can get a significant increase in specific thrust (+38%) at the expense of +40% more specific fuel consumption. At the high Mach number end of the examined flight path the thrust boost is reduced to +25% accompanied with an moderate increase of specific fuel consumption (+6%).



**Figure 6: Reheated Turbojet,  $T_3=900K$ .**

Figure 7 shows the temperature entropy diagrams at both ends of the flight path. The thrust boost of the afterburner is a result of the temperature rise from turbine exit temperature  $T_5$  to reheat exit temperature  $T_7$ . This temperature difference is much smaller at the high Mach number end.



**Figure 7: Reheated Turbojet.**

From the temperature – entropy diagrams one can also see that at the low flight Mach number much heat is added at the turbine exit pressure  $P_5$  which is significantly lower than the pressure in the main burner  $P_3$ . This is thermodynamically not desirable because the entropy rise for a given temperature difference is increasing with decreasing pressure. At the high Mach number end of the flight path there is nearly no difference between the pressures  $P_3$  and  $P_5$  and therefore the increase in specific fuel consumption due to reheat is moderate.

### 2.1.3 Ramjet

A ramjet can be considered as a degenerated reheated turbojet: one with compressor pressure ratio of 1. Figure 8 shows the comparison of such a ramjet with the reheated turbojet described in the previous section. At the top Mach number of the reheated turbojet (Mach 3.9) the specific thrust is the same for both engine configurations. The seemingly higher specific fuel consumption of the ramjet at Mach 3.9 is mainly caused by the burner efficiency differences assumed in this exercise: in the turbojet the main part of the heat addition is in the core combustor with 100% burner efficiency while the combustion in the ramjet is equivalent to that of an afterburner with 90% efficiency.

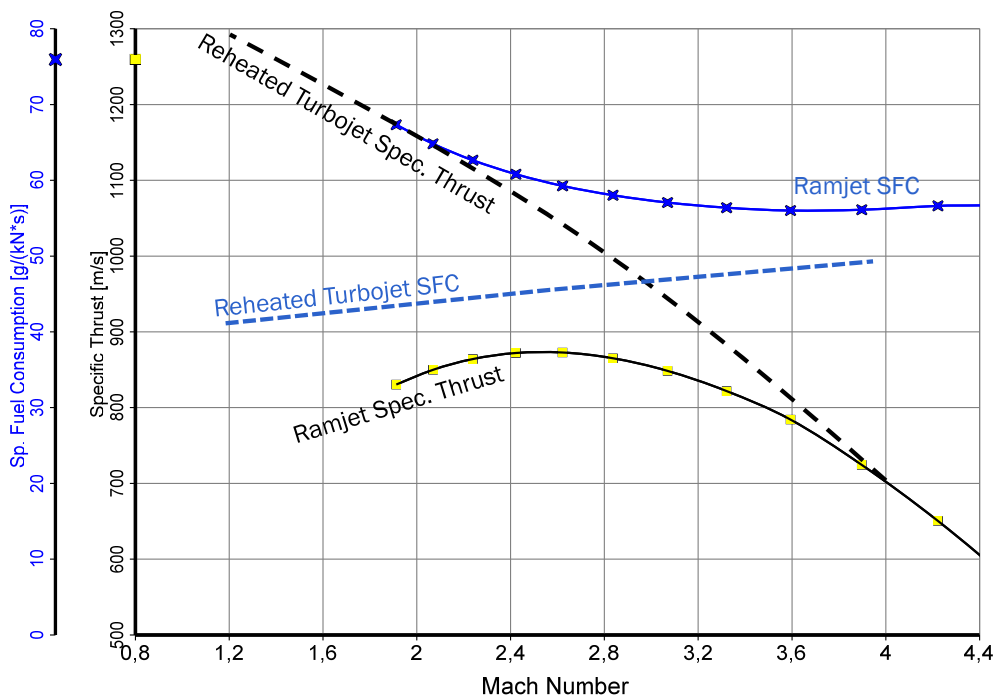


Figure 8: Ramjet.

Of course the difference between the burning efficiencies of the two engine configurations is purely academic. Along the flight path with 375knots basically there is a smooth transition from the reheated turbojet to the ramjet cycle.

## 2.2 Turbofan

Due to their high specific fuel consumption turbojets are no longer used on commercial aircraft, they have been replaced by high bypass turbofan engines. Even in modern supersonic fighter aircraft like the F-16, F-18, Dassault Rafale or the Eurofighter Typhoon are turbofan engines installed, however, these engines have a much lower bypass ratio. A low bypass engine is obviously a candidate for high speed propulsion.



### 2.2.1 “Dry” Turbofan

Figure 9 shows the schematic of a mixed flow bypass engine with a convergent-divergent nozzle. The following cycle calculations employ basically the same loss assumptions as they have been used for the turbojet. Fan pressure ratio is selected such that the total pressure at the bypass exit  $P_{16}$  is equal to the low pressure turbine exit pressure  $P_6$ . This choice guarantees favorable mixer inlet conditions.

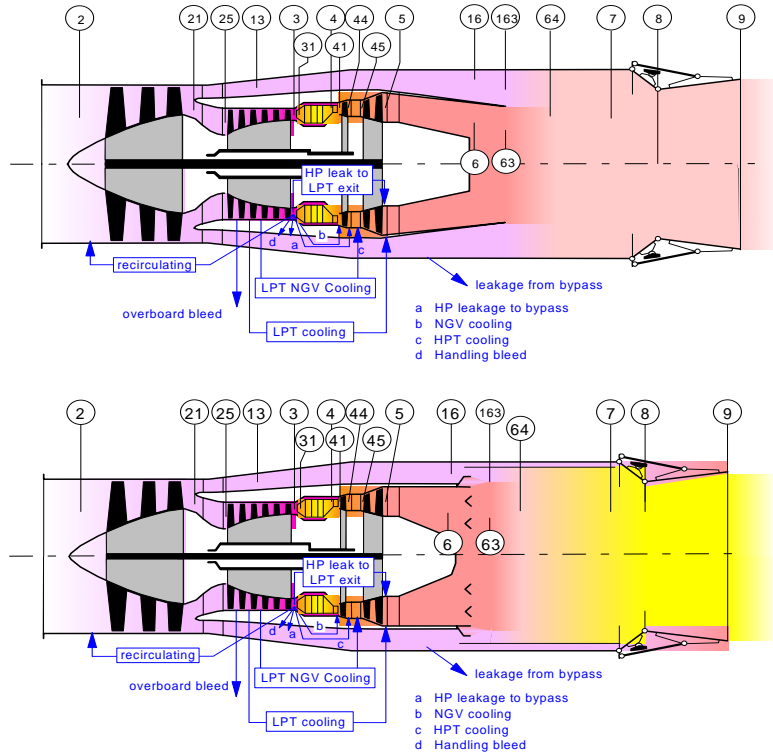


Figure 9: Turbofan Nomenclature.

Figure 10 is similar to Figure 3 which describes the dry turbojet performance for three points on the flight path with 375knots. The important difference is that instead of burner exit temperature  $T_4$  now the bypass ratio is the second parameter, the first parameter is in both cases the overall pressure ratio  $P_3/P_2$ . All turbofan engine cycles have been calculated with  $T_4=1900K$ .

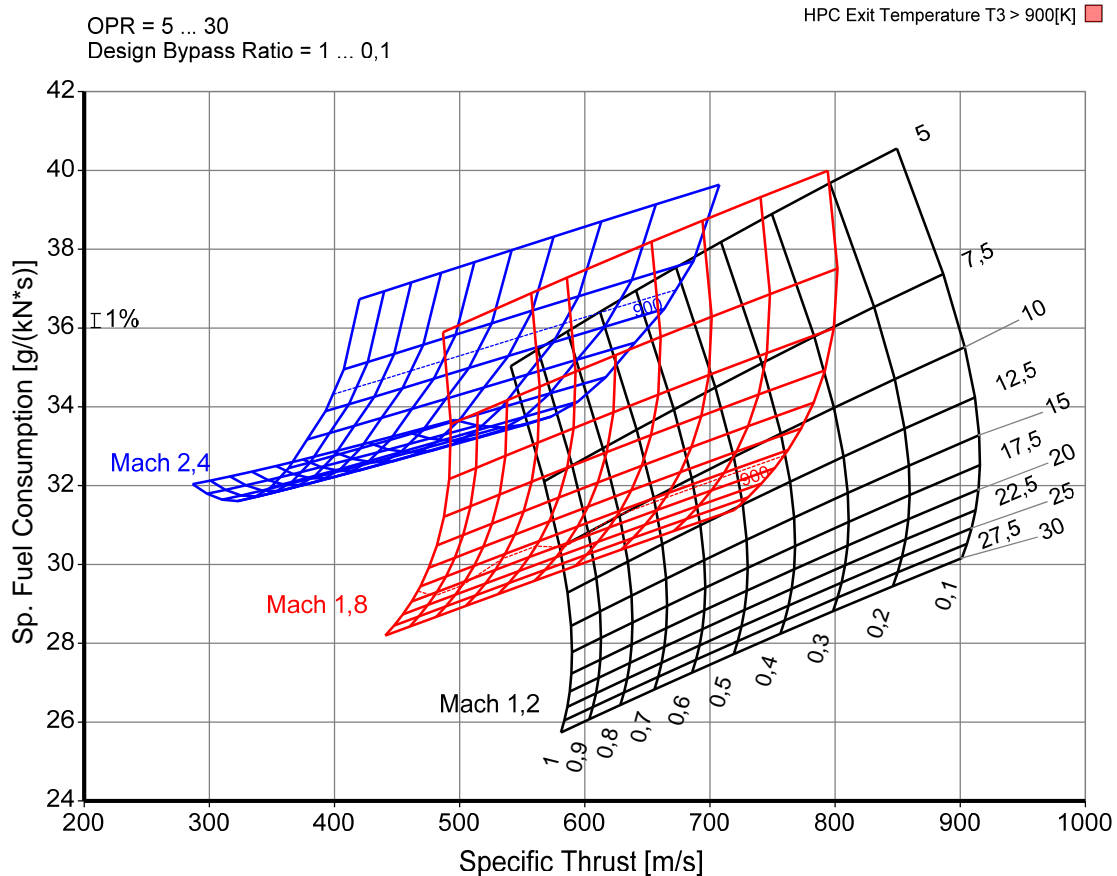


Figure 10: Dry Mixed Flow Turbofan,  $T_4=1900K$ .

Bypass ratio is varied between 0.1 and 1 and overall pressure ratio from 5 to 30. Increasing bypass ratio goes along with a very significant decrease in specific thrust and a moderate decrease in specific fuel consumption. Both effects are smaller at higher Mach numbers.

High pressure compressor exit temperature  $T_3=900K$  presents a limitation for the same reasons as for the turbojet: it is a last compressor rotor disk temperature limit because no cooling air with a lower temperature and high enough pressure is available. At Mach=1.2 the maximum permissible  $T_3$  is not achieved within the range of overall pressure ratios examined. At Mach=1.8 the overall pressure ratio is limited to ~21 and at Mach=2.4 to approximately 9 as in case of the turbojet.

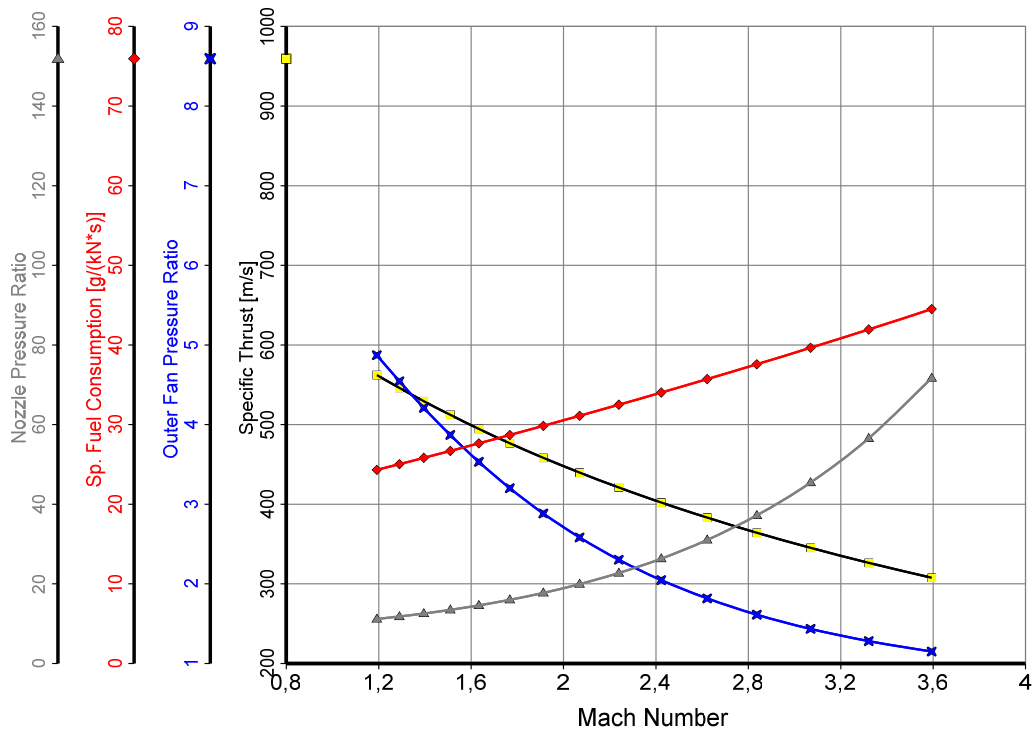


Figure 11: Dry Mixed Flow Turbofan Bypass Ratio=1,  $T_3=900K$ .

Figure 12 shows data for a turbofan with bypass ratio 1 along the 375knots flight path in comparison with those of a dry turbojet. Overall pressure ratio is adjusted in such a way that  $T_3=900K$ . Since the turbofan has an additional source of losses – those in the bypass duct – the highest Mach number is with 3.6 somewhat lower than that of the turbojet concept which did allow Mach=3.9. At the low Mach number end the turbofan decrease in specific fuel consumption of 17% is accompanied by a loss in specific thrust of 40%. At Mach=3.6 the SFC advantage is only 2.5%, specific thrust is down by 49%. It is quite obvious that at the high Mach number end the dry turbofan is not an attractive concept.

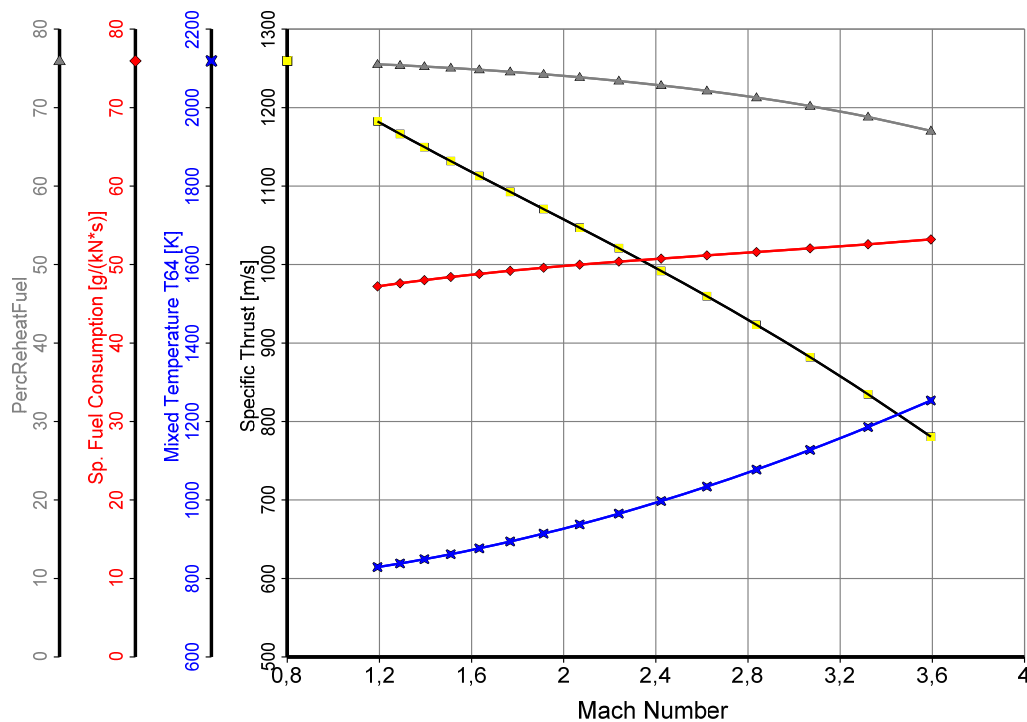


Figure 12: Reheated Mixed Flow Turbofan Bypass Ratio=1,  $T_3=900K$ .

Nozzle pressure ratio is in the range from 11 to 72 while that of the turbojet  $P_8/P_{amb}$  is between 20 and 96, see Figure 4. Jet velocity increases with nozzle pressure ratio and therefore  $P_8/P_{amb}$  can be considered as a measure of jet noise. Especially at low Mach numbers there is a clear jet noise advantage for the turbofan.

It depends on the aircraft design and its mission mix whether the SFC benefit of a dry turbofan relative to a dry turbojet overcompensates the loss in specific thrust or not. For commercial supersonic aircraft jet noise considerations will enforce the use of an engine that operates as turbofan during take off and landing.

### 2.2.2 Turbofan with Reheat

The schematic of such an engine is shown in the lower part of Figure 9. The calculation of the reheat process begins after the mixing calculation, i.e. at station 64. Thus the reheat inlet temperature  $T_{64}$  is significant lower than the low pressure turbine exit temperature  $T_6$  while the reheat inlet temperature of the reheated turbojet is equal to  $T_6$ .

Figure 12 shows data again along the 375knots flight path for engines with maximum achievable pressure ratio, i.e.  $T_3=900K$ . There is a comparatively small loss in specific thrust relative to the “wet” turbojet at Mach=1.2 which essentially disappears at the high Mach end. Specific fuel consumption of the turbofan is higher than that of the turbojet because much more heat has to be added in the relatively inefficient afterburner because the temperature difference  $T_7 - T_{64}$  is much bigger than  $T_7 - T_6$  in case of the turbojet. Another reason for the SFC delta is that the pressure in the afterburner of the turbofan is lower than that in the turbojet reheat system.

The topmost line (marked with triangles) in Figure 12 highlights the importance of the afterburner for high speed propulsion: 65% to 75% of the total fuel is burned there while in the turbojet the majority of the fuel is burned in the main combustor, see Figure 6.

Especially at the high Mach number end of the flight path a low bypass turbofan can be an attractive option because it offers SFC and noise advantages if operated in dry mode at low flight Mach numbers, take off and landing. The penalty of higher SFC in augmented mode compared to the “wet” turbojet is moderate.

### 2.3 Dry and Reheated Turbofan Size

The predominant aim for a fighter aircraft is almost always to achieve high aircraft thrust-to-weight ratio, in the interests of speed, agility and weapons carrying capability. This means engine thrust-to-weight ratio needs to be high. Even more importantly, engine thrust per frontal area must be high because this results in reduced aircraft fuselage cross-section. Any growth in engine diameter has a considerable effect on airframe size and weight.

In the following cycle study we look for turbofan engines which all deliver the same thrust. The total mass flow is adjusted in each case in such a way that the required thrust is achieved. Combustor and reheat exit temperature are held constant as well as all component efficiencies. The outer fan pressure ratio is adjusted in such a way that the total pressure ratio of bypass exit to core exit pressure  $P_{16}/P_6$  is equal to 1.0.

The Mach number at the fan inlet is 0.55 for all engines and the mixer Mach number is set to 0.18 in case of a reheated engine. This low value is necessary for two reasons, first because high velocities destabilize the flame and second because high reheat inlet Mach numbers can yield excessive fundamental pressure losses or even choking of the flow at the reheat exit. For dry engines there is no need to keep the mixer Mach number down and therefore this property is set to 0.4.

Figure 13 shows specific fuel consumption of reheated turbofans all delivering the same thrust plotted over the mixer flow area. The colored contours indicate the engine inlet area, just upstream of the compressor. In all cases the mixer area is much bigger than the engine inlet area and thus the conditions at the afterburner inlet determine the maximum engine diameter. For the overall pressure ratio of 16 the mixer area increases over the bypass ratio range 0.25 to 2 from 0.085m<sup>2</sup> to 0.108m<sup>2</sup> while the engine inlet area is in the range of 0.0578m<sup>2</sup> to 0.0615m<sup>2</sup>.

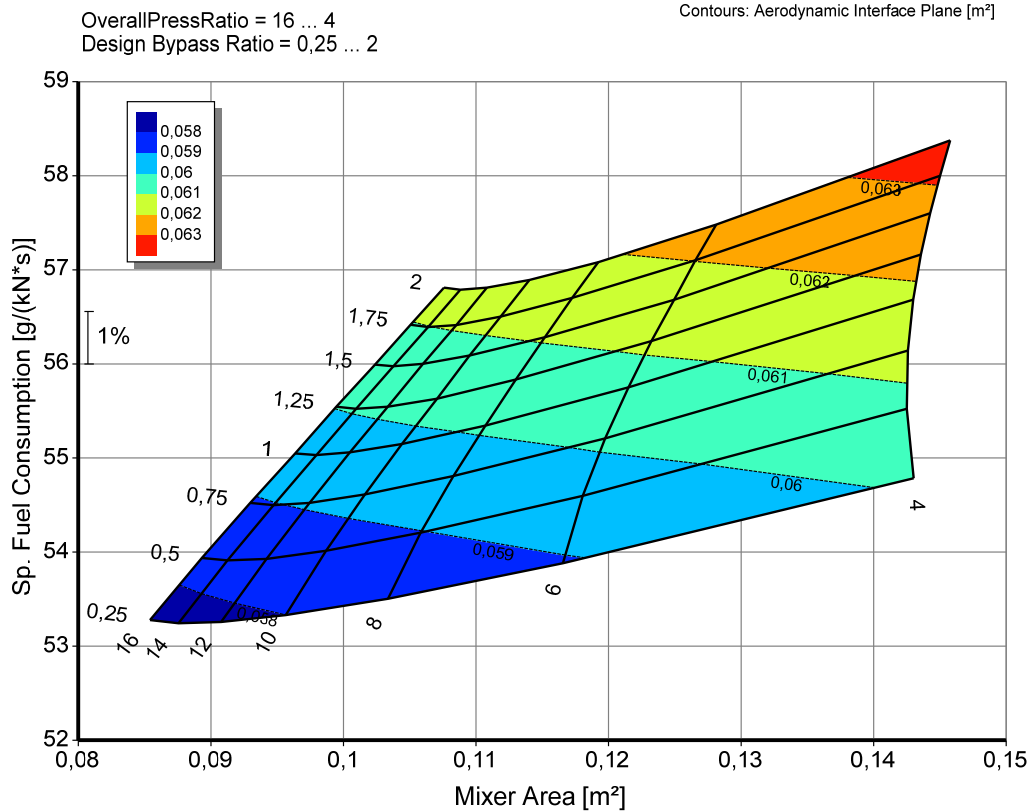


Figure 13: Reheated Mixed Flow Turbofan, Alt=13km, Mach 2.

The data shown in Figure 14 are for dry turbofans that all deliver the same thrust as the engines from the previous figure. Here we see that mixer area generally is smaller than the flow area at the engine inlet, thus the conditions at the compressor inlet determine the engine diameter. The engine inlet area increases over the range of bypass ratios considered from 0.1m<sup>2</sup> to 0.21m<sup>2</sup> because the specific thrust of the dry engine is significantly lower than that of the reheated engine. The mass flow required for the given thrust is considerably higher.

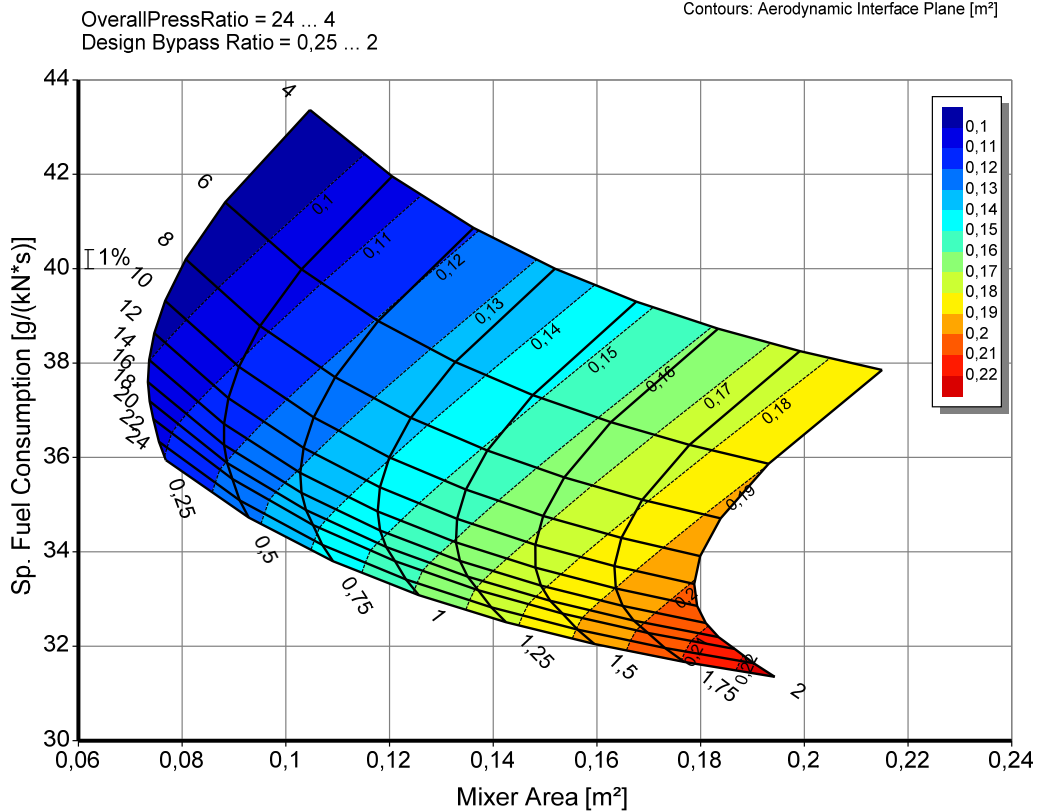


Figure 14: Dry Mixed Flow Turbofan – Alt=13km, Mach 2.

Taking the fan diameter as a measure of engine size leads to the conclusion that the dry engine frontal area is bigger (BPR=0.25: +20%, BPR=2: +100%) than that of a reheated engine with the same thrust at the flight Mach number of 2.

### 3.0 ACCELERATION TO HIGH MACH NUMBERS

All the previous examinations were comparing engines that are designed for the respective flight condition with a specified burner exit temperature, pressure ratio and bypass ratio. All efficiencies and loss assumptions were fix numbers. Consequently each calculated cycle did represent a different engine.

In the following we will select a cycle design point first and then evaluate the off-design behavior of the engine. For this off-design simulation the geometry of the gas turbine is fixed – except for the variable guide vanes the compressors might have and the adjustable nozzles needed for afterburner operation.

#### 3.1 Turbojet

For the cycle design point we select Mach 3 at an altitude of 22700m which is on the 375knots flight path examined before. With the same assumptions as made in section 2.1.2 we get the following cycle data for a reheated turbojet:

Table 1: Reheated Turbojet Cycle for Mach 3.

W T P WRstd  
Station kg/s K kPa kg/s FN = 66, 58 kN

```

amb 216,65 3,577 TSFC = 48,5250 g/(kN*s)
1 72,895 600,86 131,820 FN/W2 = 913,38 m/s
2 72,895 600,86 106,658 100,000
3 72,895 900,00 421,346 30,981 Prop Eff = 0,6789
31 63,127 900,00 421,346 eta core = 0,6495
4 65,123 1900,00 408,705 41,457
41 71,246 1821,81 408,705 44,412 WF = 1,99545 kg/s
49 71,246 1565,08 190,856 91,776 WFRH = 1,23541 kg/s
5 74,891 1535,36 190,856 91,776 WF total = 3,23086 kg/s
6 74,891 1535,36 187,039 A8 = 0,4895 m2
61 67,402 1535,36 187,039
7 68,637 2000,00 185,652 XM8 = 1,00000
8 76,126 1956,31 185,652 108,256 P8/Pamb = 51,9076
Bleed 0,000 900,00 421,346 WBI d/W2 = 0,00000
----- Ang8 = 25,87 °
P2/P1 = 0,8091 P4/P3 = 0,9700 P6/P5 0,9800 CD8 = 0,9483
Efficiencies: isentr polytr RNI P/P W_NGV/W2 = 0,08400
Compressor 0,8811 0,9000 0,439 3,950 WCL/W2 = 0,05000
Burner 0,9999 0,970 Loading = 100,00 %
Turbine 0,9075 0,9000 0,468 2,141 e45 th = 0,88691
Reheat 0,9000 0,993 XM61 = 0,18000
XM7 = 0,21438
----- far7 = 0,04621
Con-Di Nozzle: A9/A8 = 6,11924
A9*(Ps9-Pamb) -4,50E-6 CFGid = 1,00000

```

However, the engine must be able to operate not only at this conditions but also on all other points of the flight path. If we go with constant EAS=375knots down to lower Mach numbers and altitudes then the total temperature at the engine face  $T_2$  decreases from the more than 600K at the cycle design point to 278K at Mach 1.2/11000m.

For getting the highest thrust at each flight condition we want to run the engine always at its limits one of which is the rotational spool speed  $N$ . Since  $T_2$  decreases with Mach number the aerodynamic spool speed  $N/\sqrt{T_2}$  increases significantly. At the standard day temperature of 288.15K the aerodynamic spool speed would be higher than at the cycle design point by a factor of  $\sqrt{600.9/288.15}=1.444$  if the rotational spool speed  $N$  is held constant. (If the cycle design point would be at Mach=3.9 then the factor would be even 1.73).

For the compressor that means, that at the cycle design point there must be an aerodynamic overspeed margin of around 45% if unrestricted operation along the flight path is to be achieved. Applying the usual compressor design rules, however, will yield only 5 to maximum 10% aerodynamic overspeed margin. Consequently the aerodynamic design of the compressor must be done at a much higher pressure ratio and higher corrected flow than found at the cycle design point. How big the pressure ratio difference between the cycle design point and the aerodynamic design point of the compressor needs to be depends on the mission of the air vehicle to be designed.

The cycle design pressure ratio is approximately 4. Two alternate compressor design points are examined, one with a compressor design pressure ratio of  $\Pi_{DS}=7$  and another one with  $\Pi_{DS}=10$ . The engine performance is examined along a mission segment with EAS=375knots between Mach numbers of 1.2 at an altitude of 11km and Mach 3, altitude 22.7km.

Figure 15 shows the operating line of the compressor designed for  $\Pi_{DS}=10$  and Figure 16 that of the alternate design. Note that there is a significant size difference between both compressors, the Standard Day corrected mass flow is 150kg/s for the  $\Pi_{DS}=7$  machine and 205kg/s for the other one. At the cycle design point - marked by a circle on the  $N/\sqrt{\Theta}=1$  line - both compressors operate with nearly the same corrected flow and pressure ratio.



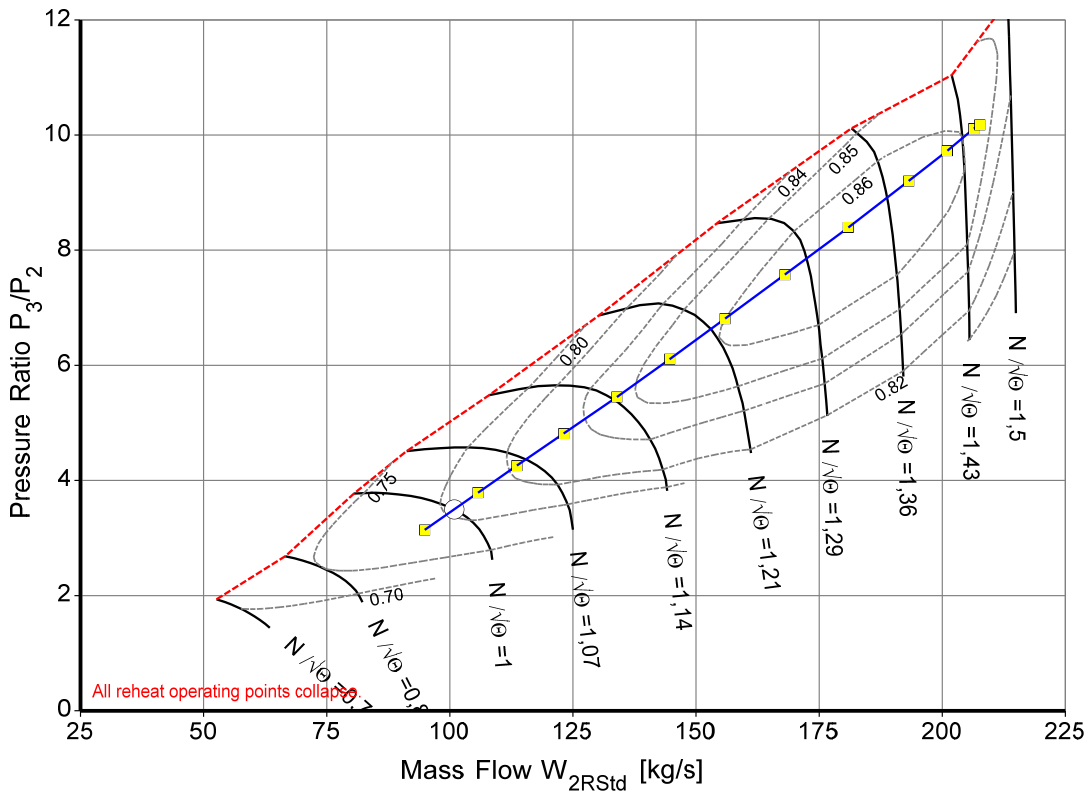


Figure 15: Compressor Design 1:  $\Pi_{DS} = 10$ .

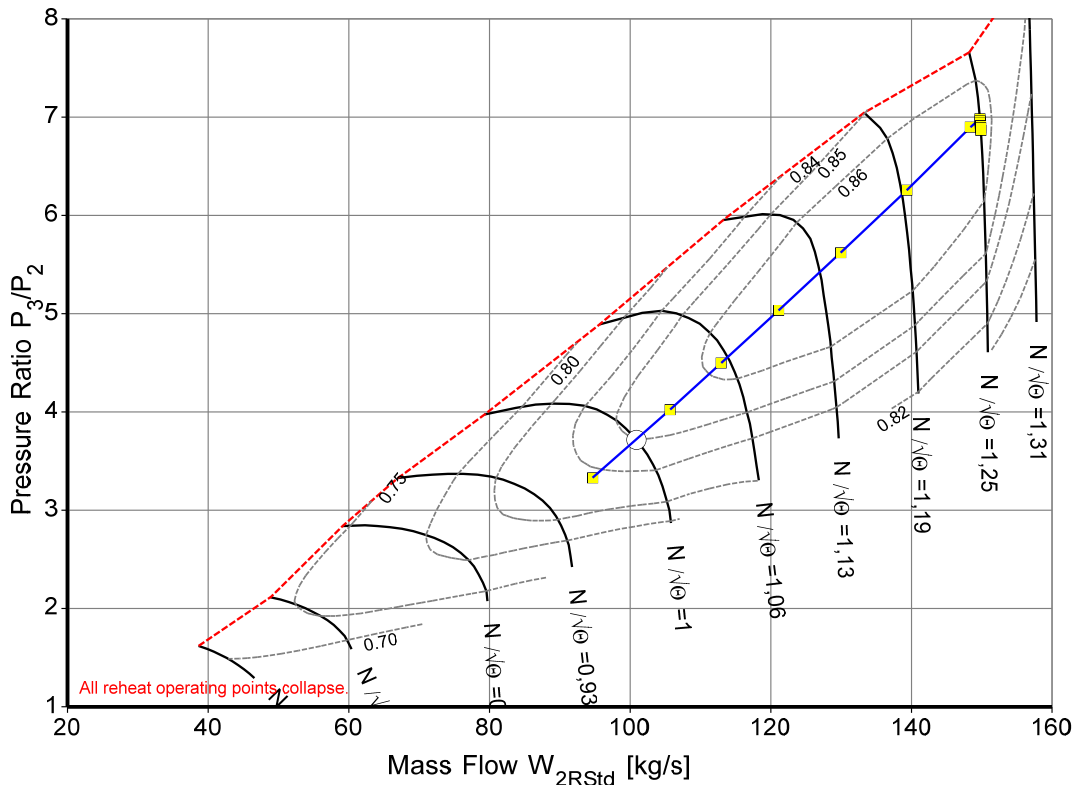


Figure 16: Compressor Design 2:  $\Pi_{DS} = 7$ .

Why are the operating points at the cycle design conditions not identical? The reason is that there is a compressor efficiency difference. At the compressor design point there is only a very small efficiency difference: Compressor 1 ( $\Pi_{DS}=10$ ) has  $\eta_{DS}=0.859$  and compressor 2 ( $\Pi_{DS}=7$ ) shows  $\eta_{DS}=0.861$ . However, compressor 1 operates at conditions farther away from its design point and therefore the operating efficiency is only 0.80 while compressor 2 ( $\Pi_{DS}=7$ ) operating nearer to its design point picks 0.85 from the map at the Mach 3 operating point, the circle.

It looks like that all advantages are on the side of compressor 2, that, however, is a bit shortsighted. Note that in Figure 16 at the top end of the operating line many points collapse. This is because in the simulation the control system prevents operation at corrected speeds  $N/\sqrt{\Theta}$  greater than 125% of that at the cycle design Mach number.

Figure 17 shows how all controlled parameters behave along the flight path. The symbols on the axes and the various lines make them distinguishable. Turbine stator outlet temperature  $T_{41}$  is limited to 1822K which corresponds to the design burner exit temperature  $T_4=1900K$ . Maximum permissible relative HPC Spool Speed ZNX is 1.0 and compressor exit temperature  $T_3$  must not exceed 900K. The big difference between the two compressor variants is in the corrected spool speed limitation which is 1.45 (compressor  $\Pi_{DS}=10$ ) respectively 1.25 (compressor  $\Pi_{DS}=7$ ).

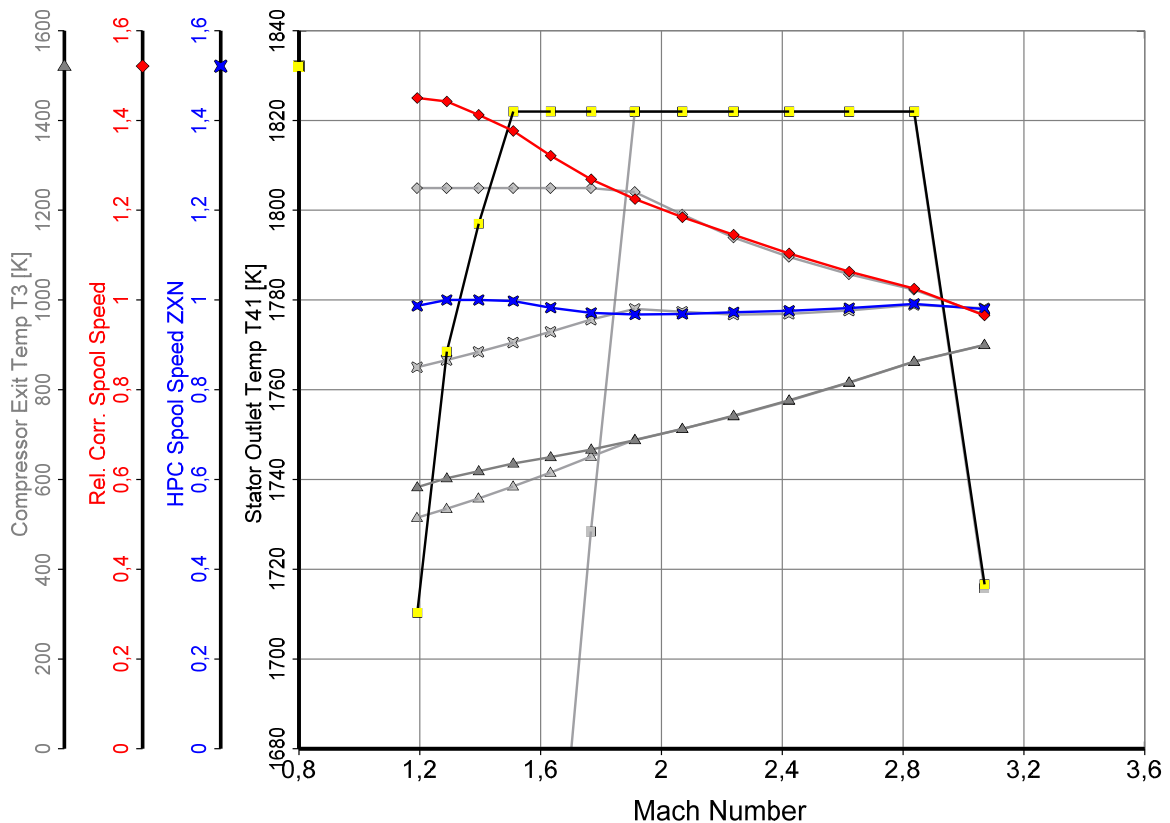


Figure 17: Engine Control - Background Lines for Compressor Design 2 ( $\Pi_{DS} = 7$ ).

At the high speed end the  $T_3$  limiter is just touched which depresses the other controlled parameters slightly for both engine design alternatives. The machine with the compressor design pressure ratio of 10 operates at the  $N/\sqrt{\Theta}$  limiter only at Mach 1.2; the relative HPC spool speed limit of 1.0 is active in the

Mach number range from 1.3 to 1.5. At all other Mach numbers the maximum permissible turbine temperature  $T_{41}$  limits the performance of this engine.

The machine with the smaller compressor operates at the  $N/\sqrt{\Theta}$  limiter at all Mach numbers below 1.9 and that has a distinct affect on the performance as can be seen in the next two figures. For the reheated engine (Figure 18) the thrust loss of up to 35% is accompanied by an increase of specific fuel consumption of 12%. The dry turbojet (Figure 19) loses also up to 48% thrust due to the severe  $N/\sqrt{\Theta}$  limitation, however, specific fuel consumption improves by 7%.

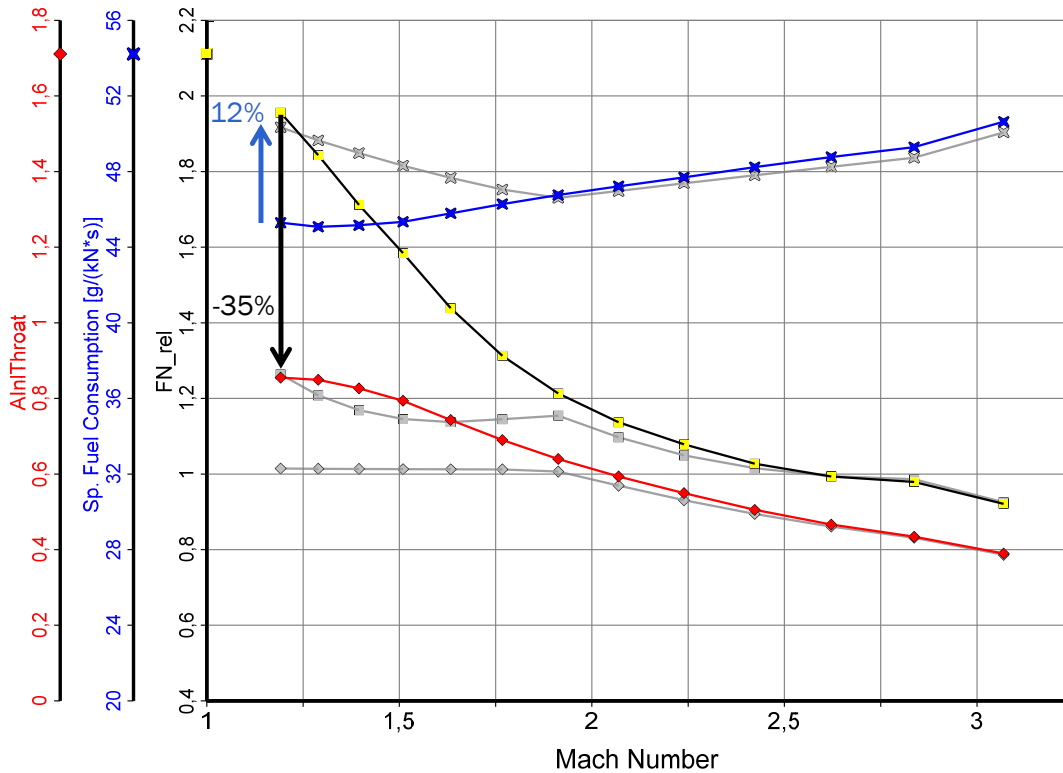


Figure 18: Reheated Turbojet – Background Lines for Compressor Design 2 ( $\Pi_{Ds} = 7$ ).

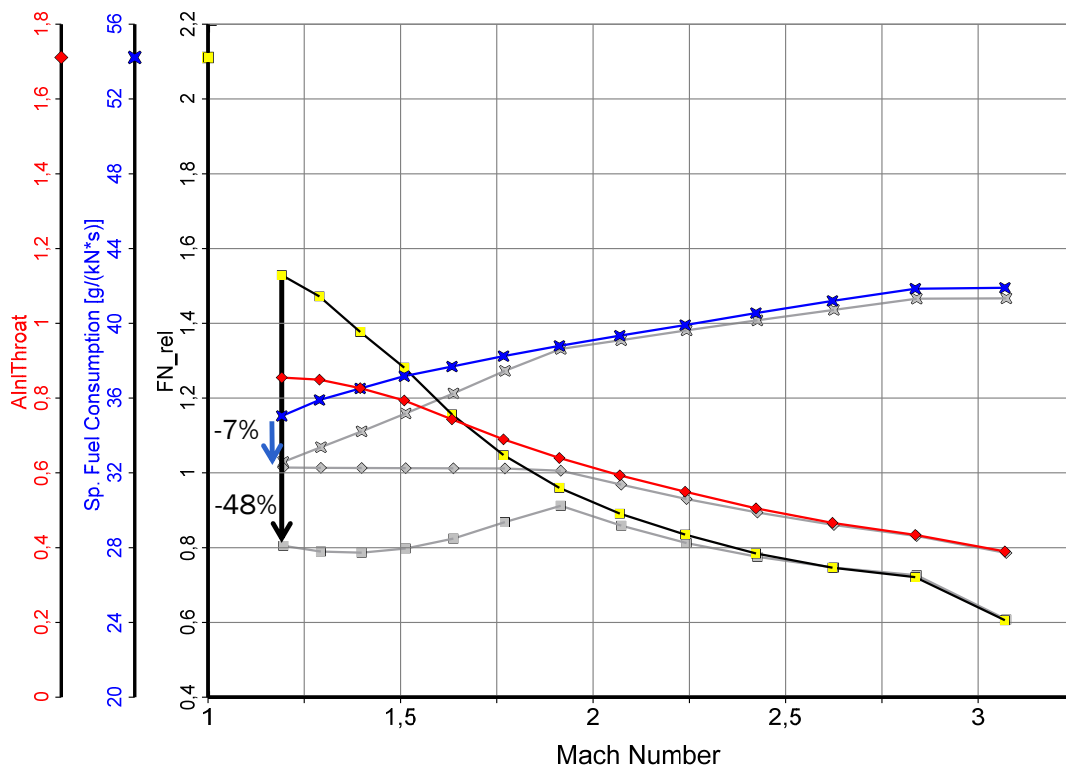


Figure 19: Dry Turbojet – Background Lines for Compressor Design 2 ( $\Pi_{DS} = 7$ ).

In Figures 18 and 19 there is one more parameter shown that has not yet been explained:  $A_{InlThroat}$ . This quantity is an indicator for the aircraft intake throat area, calculated by employing engine inlet total pressure  $P_2$  and temperature  $T_2$  as well as the engine mass flow  $W_2$  assuming sonic flow. The first important message of this indicator is that the aircraft engine intake needs to have variable geometry for adjusting the flow area to the mass flow of the engine. The second message is, that with the bigger compressor ( $\Pi_{DS}=10$ ) the variability of the aircraft intake needs to be nearly twice as big as with the smaller compressor ( $\Pi_{DS}=7$ ).

The rather simple control system employed for this study could be improved by making use of the variable geometry features that are required for such an engine anyway. With the variable guide vanes of the compressor one can influence the relationship between mass flow and spool speed as long as they are not fully open. This is the case for all operating points that are not affected by the  $N/\sqrt{\Theta}$  limiter. Thus it might be possible to improve performance at flight conditions where the rotational spool speed limiter is hit.

Another fine trim for the engine operation could be a sophisticated nozzle area schedule: one needs not necessarily to operate both for dry and reheat the compressor at the same point in the map as assumed here. Moreover nozzle throat area can be made a function of flight conditions and corrected spool speed. That would not only affect compressor surge margin but also burner exit temperature at a given mass flow.

Which engine design is to be preferred depends on the mission of the aircraft. What the thrust requirements are at each Mach number will decide about the optimum compressor design mass flow and pressure ratio. Also aircraft intake design aspects will play a role in the final selection of the engine configuration. Thus the mission defines the cycle.

### 3.2 Variable Cycle Engine (VCE)

The previous section has discussed how the flight mission affects the choice of the compressor design point of a turbojet engine. Similar studies could be performed for dry and reheated turbofan engines. There certainly would be some additional arguments, however, nothing fundamentally new. Therefore we skip the low bypass turbofan engine type and proceed with some thoughts about variable cycle engines.

Variable cycle engines are potentially attractive for aircraft which have to fulfill a mix of subsonic and supersonic missions. The aim of the engine design is to combine the advantages of the turbojet (high specific thrust) with that of a turbofan (low specific fuel consumption, low noise).

Many different variable cycle engine configurations have been studied in the past. Ref. 4 gives an overview about the work done at General Electric Aircraft Engines. The architecture of the VCE proposed by GEAE for the Advanced Tactical Fighter ATF is shown in Fig. 20. An engine of this configuration, the F120, has successfully flown in both the YF22 and YF23 ATF prototype aircraft.

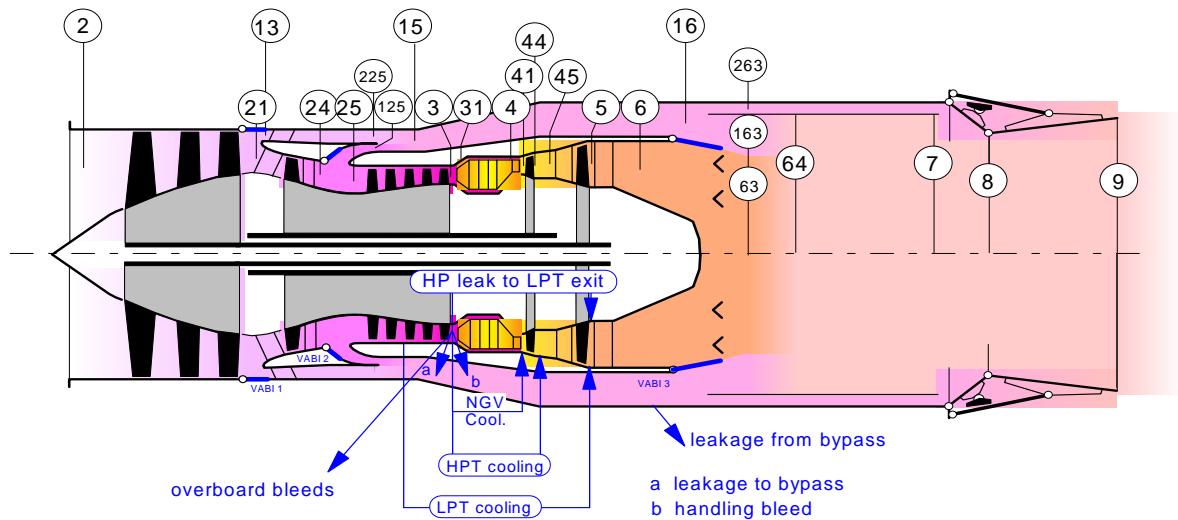


Figure 20: Variable Cycle Engine Nomenclature.

For evaluating some typical performance characteristics of this type of VCE a cycle with the following main parameters at ISA SLS is considered:

Table 2: Main Cycle Data for a VCE Example.

Dry Thrust	73.6 kN
SFC	20 g/(kN*s)
Mass Flow	100kg/s
Fan Pressure Ratio (Bypass)	3.9
Fan Pressure Ratio (Core)	3.0
Core Driven Fan Stage Pressure Ratio	1.3
HPC Pressure Ratio	6.0
Overall Pressure Ratio	23
Burner Exit Temperature	1900K
Bypass Ratio W16/W21	0.75
Bypass Ratio W16/W25	1

The engine has three so-called variable bypass injectors (VABI). The first VABI is a selector valve downstream of the fan which allows closing the bypass inlet. The second VABI is again a valve which is located between the core driven fan stage (CDFS) and the inlet to the HP compressor. The third VABI is

sort of variable area bypass nozzle which injects the secondary flow into the core stream behind the low pressure turbine.

Besides the three VABI's there are at least two more variable geometry elements in this VCE: the inlet guide vanes to the CDFS and the nozzle. The latter must be variable anyway since the engine has got an afterburner for the high supersonic part of the mission.

The following cycle studies are limited to a single dry operating point at supersonic cruise conditions with Mach 1.4 and altitude 11km. At this flight condition it is examined how the variable geometry settings - especially those of the three VABI's - affect the performance and operability of the engine. Engine rating is limited by both the design burner exit temperature  $T_4$  and the nominal HP spool speed.

Figure 21 shows how the two front VABI's affect the engine bypass ratio  $W_{16}/W_{21}$ . While VABI 1 (downstream of the fan) is open, both the nozzle area (varied in the range from nominal to +10%) and VABI 3 have a certain influence on bypass ratio. If VABI 1 is closed then the bypass ratio is nearly constant.

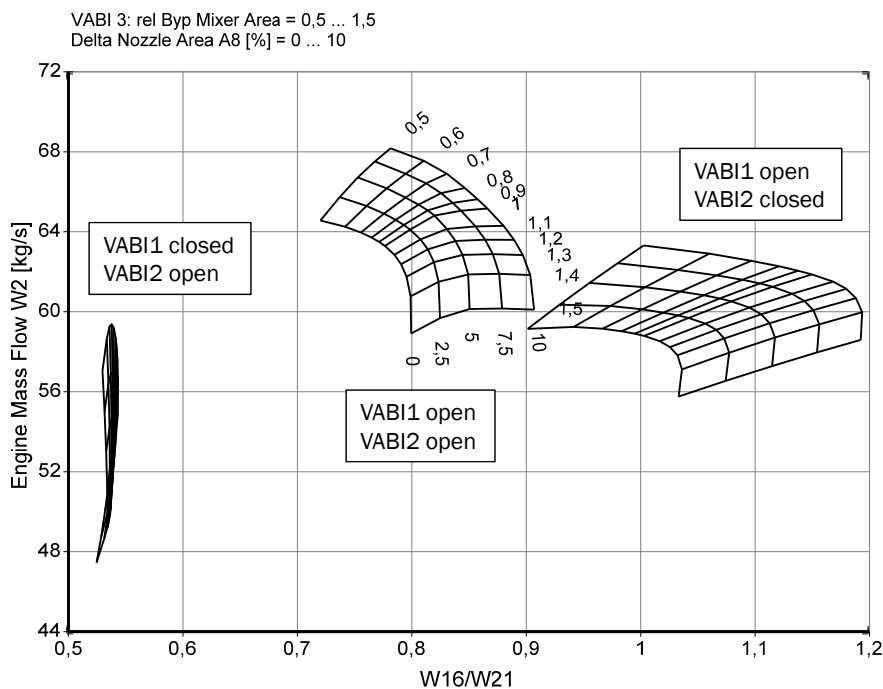


**Figure 21: Variable Cycle Engine Rear VABI and Nozzle Area Effect on Flow and Bypass Ratio.**

The numbers describing the VABI 3 position are in the range from 0.5 to 1.5. Values lower than one indicate that the bypass mixer area  $A_{163}$  is smaller than its nominal value. For example VABI 3 = 0.5 means that the bypass mixer area is reduced to 50% of the design point value. VABI 3 values bigger than one mean that the core mixer area  $A_{63}$  is reduced. A 50% reduction of  $A_{63}$  is described with VABI 3 = 1.5, for example. The sum of  $A_{163}$  and  $A_{63}$  is always equal to the total mixer area  $A_{64}$ .

Figure 22 shows the specific fuel consumption for the various geometry positions. These results are somewhat surprising since the lowest SFC is achieved with the lowest bypass ratio and the highest SFC goes with the highest bypass ratio. This result is affected by the engine rating limiters:

- If VABI 1 is open and VABI 2 closed (this VABI setting makes the engine a conventional turbofan), then the engine is limited by the HP spool speed –  $T_4$  is much lower than in the other cases.

- If VABI 1 is closed and VABI 2 open, then the active limiter is the burner exit temperature and the HP spool speed is much lower than in the other cases.
- If both VABI 1 and VABI 2 are open then the engine operates with big nozzle and bypass mixer areas at the spool speed limiter, otherwise at the temperature limit.

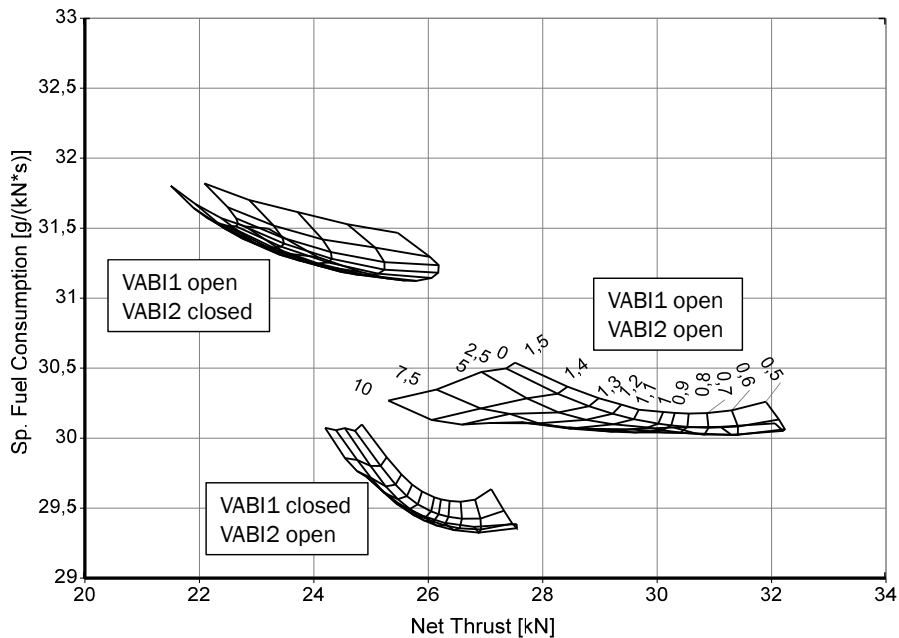


Figure 22: Variable Cycle Engine Rear VABI and Nozzle Area Effect on SFC and Thrust.

With other control schedules and also for other flight conditions the SFC picture will be different and therefore one cannot derive generally valid conclusions about the fuel consumption of this type of engine from Figure 22.

One claimed advantage of the VCE is that it can vary thrust without changing mass flow which allows for optimum flow conditions at the aircraft intake during supersonic flight. One can adapt the mass flow in such a way that the intake operates at the most favorable pressure recovery and without or reduced spillage drag.

From Figure 23 one can read at constant mass flow (~60 kg/s) a thrust range of more than 15 to 20%. Low thrust is connected with big bypass mixer and nozzle areas, high thrust with small areas.

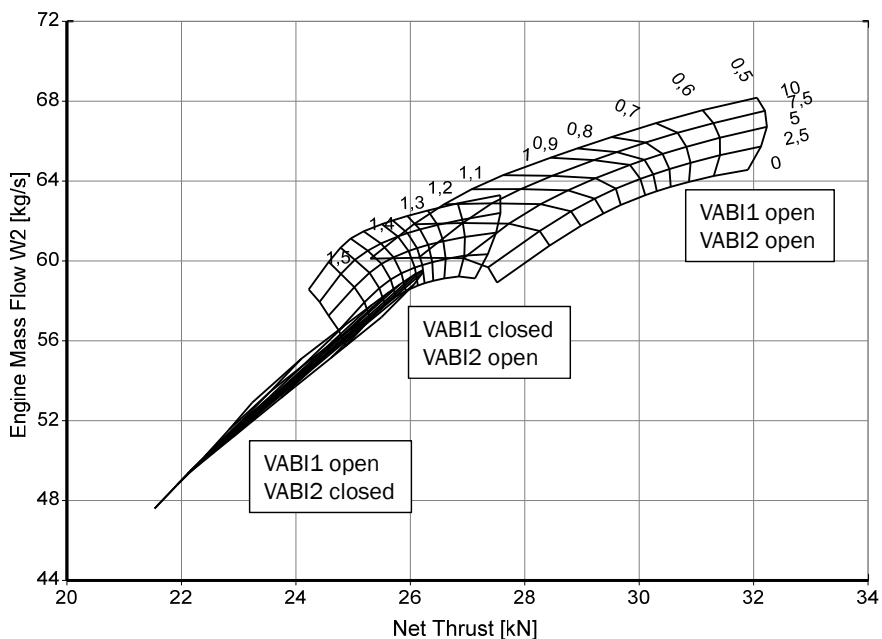
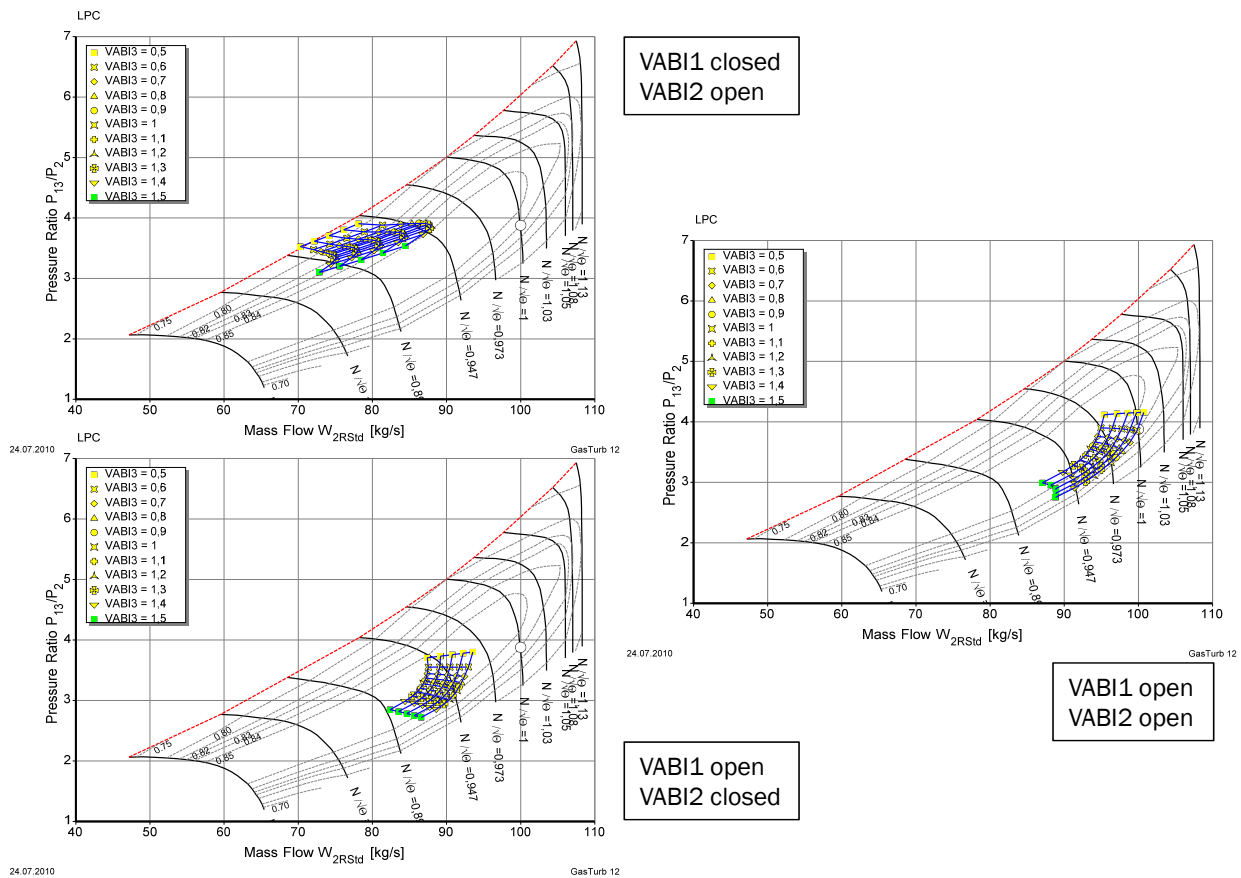


Figure 23: Variable Cycle Engine Rear VABI and Nozzle Area Effect on Flow and Thrust.

The next four figures show the operating conditions in the component maps for the various VABI and nozzle positions. The circle on the speed lines  $N/\sqrt{\Theta}=1$  mark the ISA SLS operating point with all VABI's open.

In the fan map the three operating areas (VABI 3 and nozzle area range as before) are clearly separated from each other. A sophisticated engine control system is required which schedules mixer and nozzle areas in such a way that the engine performance is optimal and sufficient surge margin is maintained.





**Figure 24: Variable Cycle Engine Rear VABI and Nozzle Area Effect on Fan Operating Point.**

Figure 25 shows three maps of the core driven fan stage CDFS. Within the operating range corrected flow varies between 18kg/s and 36kg/s - about 100%. Such a broad operating range can only be achieved with variable inlet guide vanes (IGV's). In the calculated example the IGV's are opened by 35° when VABI 1 is closed and all the engine mass flow enters the core. In contrast, when VABI 1 is open, then much less flow approaches the CDFS and the IGV's need to be closed by -25°. Altogether the IGV operating range must be 60° which is quite an aerodynamic and mechanic compressor design challenge.

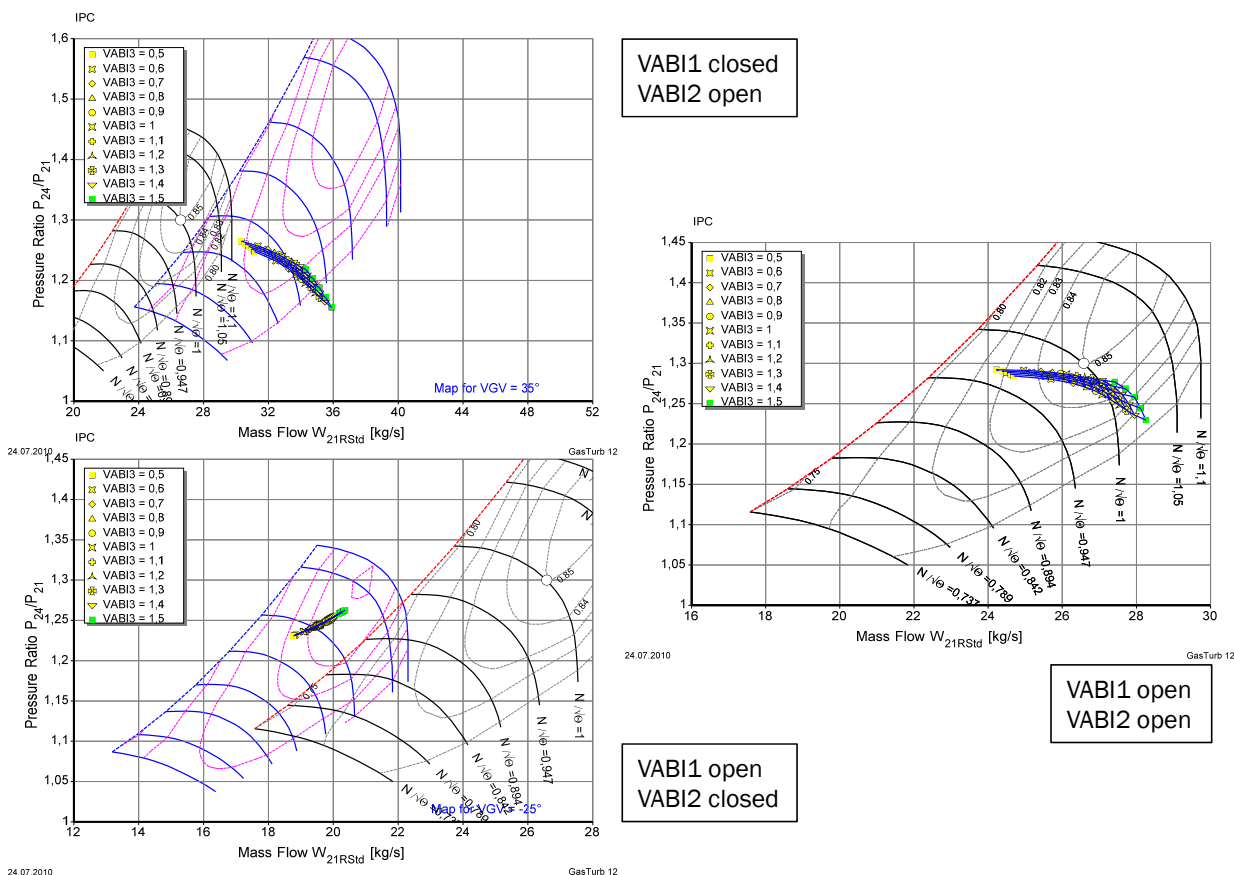


Figure 25: Variable Cycle Engine Rear VABI and Nozzle Area Effect on CDFS Operating Point.

When VABI 2 is closed then the slope of the CDFS operating line is positive in contrast to the cases with the other VABI positions. This is to be expected because in this case the stage can be considered as part of the core compressor whose operating line cannot be affected by nozzle area changes from principle.

Note also that varying nozzle area has no effect on the CDFS operating point while VABI 2 is closed and only a minor effect in the other cases. With open VABI 2 increasing the bypass mixer area yields higher surge margin.

Figure 26 shows the HP compressor operating lines – they look as those from any other gas generator compressor. The HP turbine maps are not presented – there all operating points nearly collapse and have the same pressure ratio as theory requests. In the LP turbine map (Fig. 27) all operating points are in the area of high efficiency and therefore this component does not pose a problem.

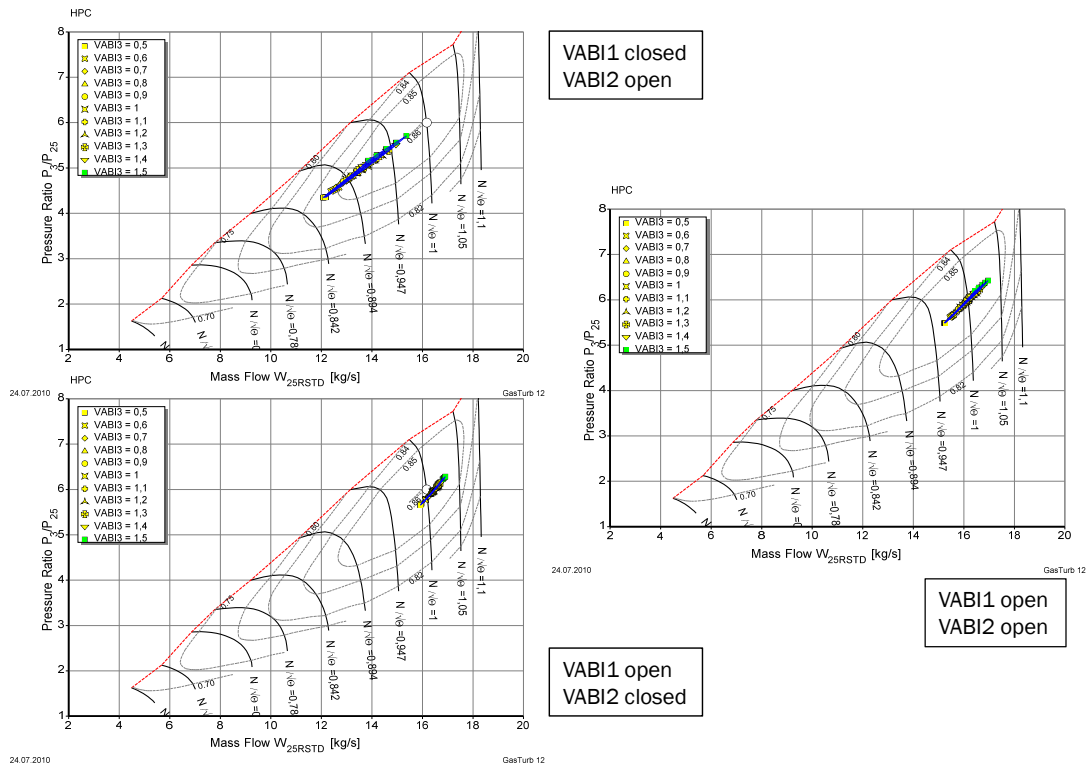


Figure 26: Variable Cycle Engine Rear VABI and Nozzle Area Effect on HPC Operating Point.

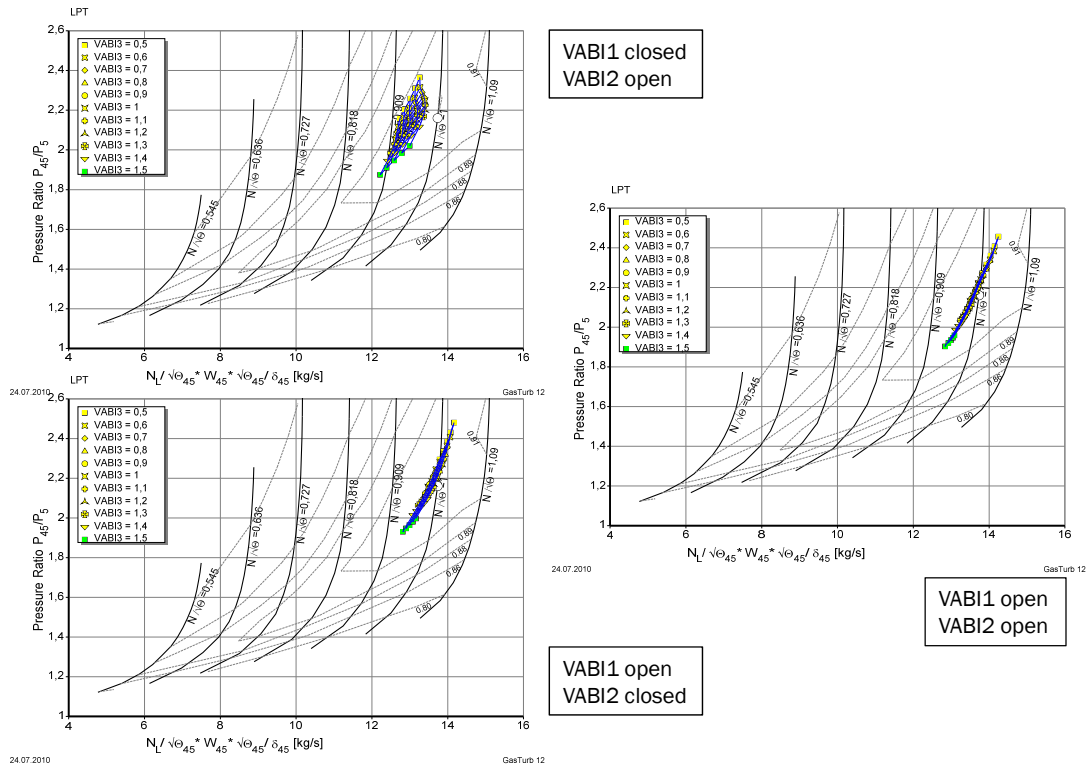


Figure 27: Variable Cycle Engine Rear VABI and Nozzle Area Effect on LPT Operating Point.

This was a short study about the maximum performance of a VCE at a single operating point. In a real world examination many more operating conditions need to be considered and finding the best propulsion system compromise between the conflicting requirements of a multi-mission aircraft is quite a challenge. Having more variable geometry allows a better adaptation of the engine to the various requirements. However, all these variable elements need to be controlled and maintained in service. In the end a simpler engine might be the better solution.

## 4.0 COMPONENTS FOR SUPERSONIC PROPULSION

### 4.1 Inlet

The higher the flight speed, the more important becomes the performance of the intake for any propulsion system of a supersonic aircraft, see Figure 7. Aircraft flying faster than around Mach 1.5 need variable geometry because otherwise the mass flow of the intake does not fit to the mass flow the engine needs for producing adequate thrust. Mismatch between intake and engine can produce excessive spillage drag (if the engine cannot swallow the mass flow delivered) or severe inlet flow distortion.

How complex the installation of a high speed engine in a supersonic aircraft is can be seen from Figures 28 and 29. These show the operating modes of the SR-71 Blackbird propulsion system which is designed for flying at Mach 3.2 in an altitude of around 80000ft (24.4km).

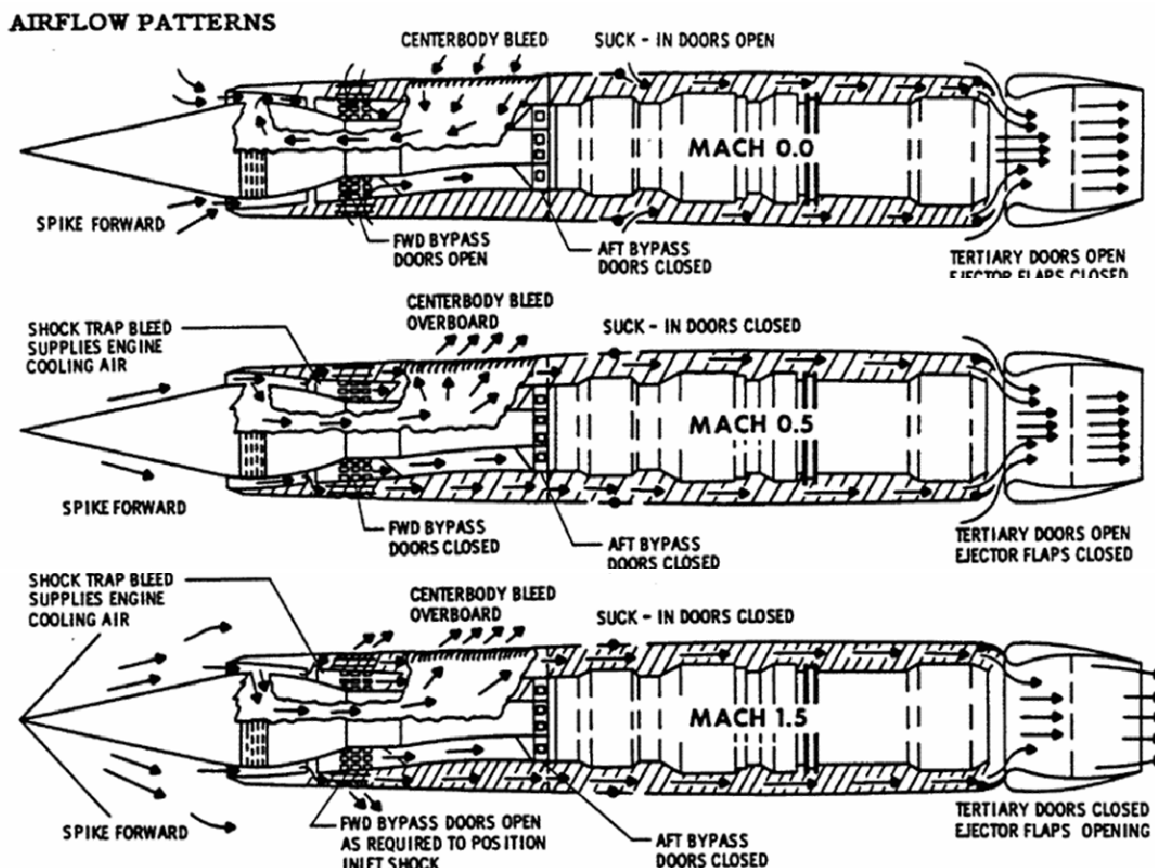
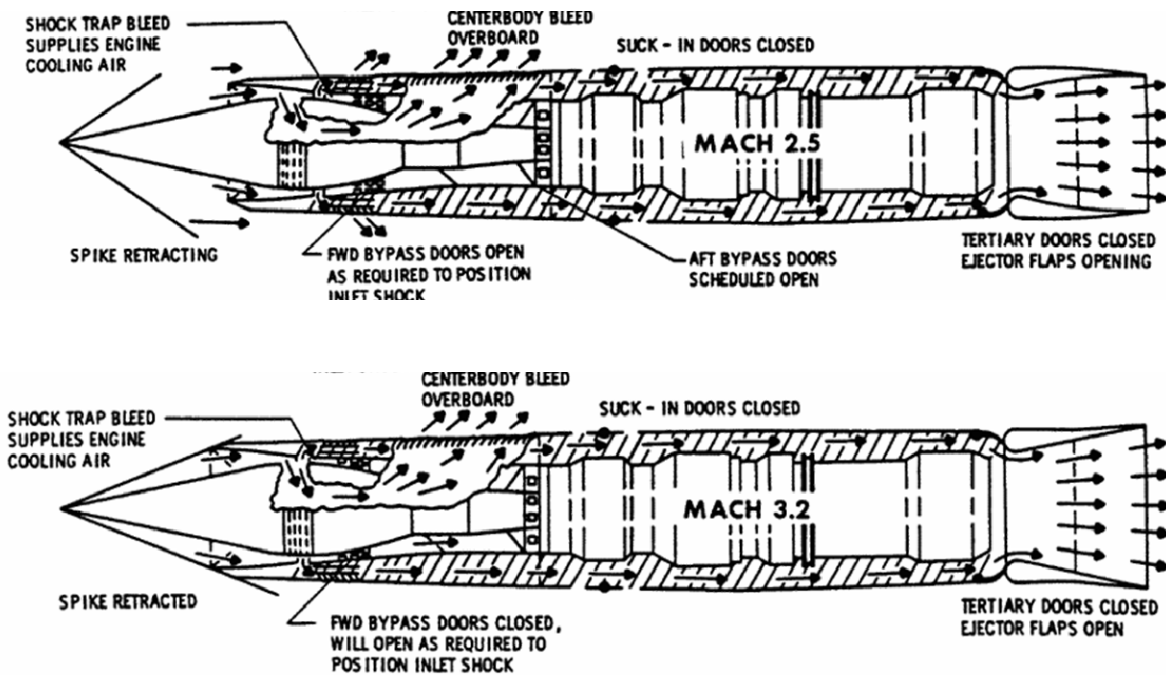


Figure 28: SR-71 Propulsion System.



<http://www.sr-71.org/blackbird/manual/1/1-33.php>

Figure 29: SR-71 Propulsion System.

Usually the intake is part of the aircraft and supersonic inlet design is a discipline on its own. In spite of its importance for the performance and operability of the overall propulsion system we will not go in more detail here and concentrate instead on two components found only in engines for supersonic aircraft, the afterburner and the variable area convergent-divergent nozzle.

## 4.2 Afterburner

An afterburner is a fairly simple device, and it consists of only a few basic parts: fuel injectors, flame-holders and a jet pipe in which the combustion takes place. A liner controls the afterburner cooling air distribution and provides cooling air to the nozzle.

Flame-holders are needed to stabilize the flame in the relatively high velocity environment. If the turbine exit temperature allows, then circular flame-holders as shown in Figure 30 can be used. The two v-shaped rings (gutters) are interconnected with a single radial gutter which allows the flame to propagate from the primary zone to the two rings during light up.

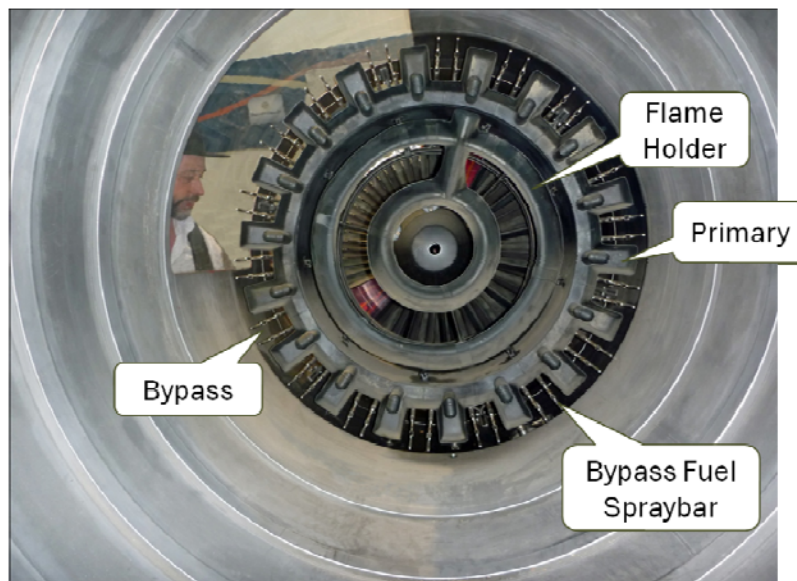


Figure 30: RB199 Afterburner.

With modern low bypass engines the temperature downstream of the LPT is so high that the flame-holders require cooling. Guiding the cooling air from the bypass through the flame-holders requires that these are of radial design like in case of the EJ200, see Figure 31. With such a design it must be sure that, while the afterburner is lit, the pressure in the bypass is always high enough to drive the cooling air through the flame-holders.

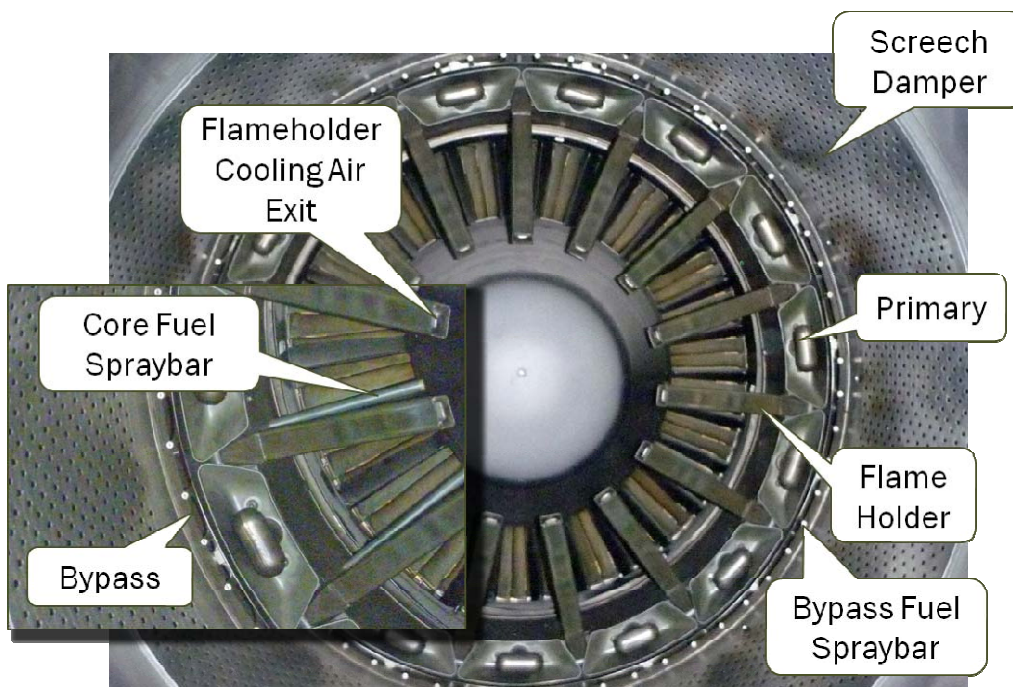


Figure 31: EJ200 Afterburner.

A screech damper is necessary to suppress high-energy destructive acoustic frequencies. The screech damper is part of the liner that protects the case from high temperatures. Through the rather big holes in

the screech damper some of the air from behind the liner will flow into the jet pipe. The amount of this air luckily increases automatically with the amount of heat released because the increasing Mach numbers in the jet pipe lead to a decreasing static pressure in the burning zone.

An afterburner must operate over a wide range of conditions. To obtain the maximum thrust the fuel must be injected in such a way, that all of the available oxygen in the main stream is burnt. That means that the fuel-air-ratio must be very uniform at the nozzle inlet. When the fuel is not distributed evenly then there are some regions that lack fuel and others with an over-stoichiometric fuel-air-ratio. In both regions the heat release is less than maximal.

At minimum afterburner rating the local fuel-air-ratio must be stoichiometric in the now small combustion region to prevent the flame from being blown out. In other words, the fuel must now be distributed very unevenly throughout the afterburner.

The afterburners of the RB199 and the EJ200 use so-called “Primaries” for the operation at minimum reheat rating. They are ignited with a hot shot device which injects locally in the main combustor some additional fuel and thus sends a flame through the turbines to the primaries.

During reheat partload the fuel is only injected into the core stream because there the combustion conditions are best. When all the oxygen in the core stream is consumed, then additional fuel is injected into the bypass stream. Note that with low bypass engines only about half of the bypass air can be used for burning, the rest is needed for cooling the liner and the nozzle.

Reheat burning efficiency is significantly lower than in the main burner and depends mainly on three parameters: the amount of fuel injected, the static pressure in the jetpipe and the bypass ratio.

- The correlation between the injected fuel-air-ratio and efficiency describes primarily the quality of the fuel-oxygen distribution (Fig. 32).
- Low pressures negatively affect the fuel droplet size because low gas pressure is always connected with small amounts of fuel (Fig. 33).
- High bypass ratios go – for a given engine geometry – with high velocity respective low residence time in the burning zone (Fig. 34).

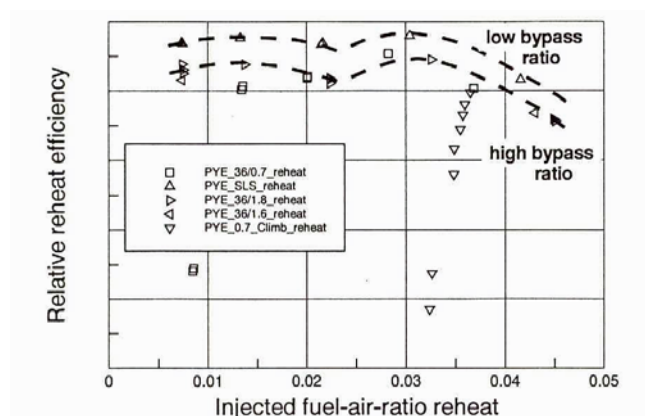


**Figure 32: Reheat Efficiency=f(FAR<sub>inj</sub>).**

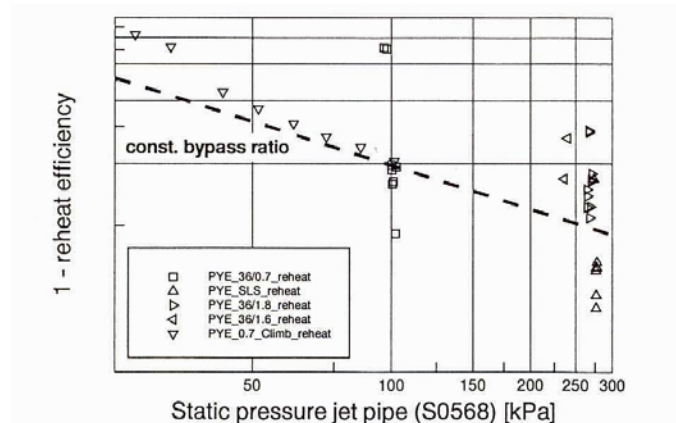


Figure 33: Reheat Efficiency= $f(P_s)$ .

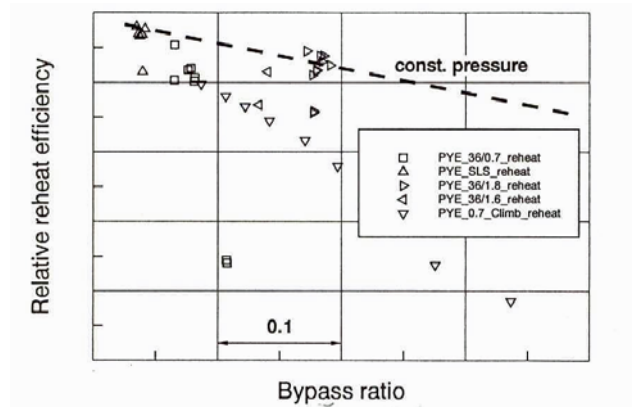


Figure 34: Reheat Efficiency= $f(BPR)$ .

The figures are taken from ref.7 which describes the background of these empirical correlations.

While the afterburner is operating, the density of the hot gases approaching the nozzle is significantly lower than with dry operation. If the nozzle throat area would not be increased while fuel burns in the afterburner, then the nozzle inlet pressure would rise. This pressure rise would travel upstream through the bypass and cause the fan to surge. Preventing this requires that the nozzle throat area and the amount of reheat fuel must be coordinated carefully. There are two basically different afterburner control philosophies:

- 1) With a closed loop control the nozzle throat area is adjusted in such a way that the scheduled fan pressure ratio is achieved.
- 2) With an open loop control the amount of afterburner fuel is calculated from the measured nozzle position and other sensed parameters.

The main difference between these two approaches is their reaction to a failure to light up or a flame out event. If the flame out event is not detected, then with the first control philosophy the nozzle will close with the aim to achieve the target fan pressure ratio. Not burning fuel is continuously injected, but it does not release any heat. If then due to a random effect the fuel suddenly ignites, then the fan will surge because the nozzle is unable to open quick enough. The use of a light-up detector is necessary to make such a control system work.



With the second control philosophy in case of an undetected failure to light up the engine will loose thrust because the nozzle pressure will be low. There is never a danger of fan surge - even with delayed ignition – because the nozzle throat area is never too small for the amount of heat released. The light-up detector will be used to cancel the fuel supply and then close the nozzle to regain at least the dry thrust of the engine.

Traditionally the first control philosophy is used in the US while both the RB199 and the EJ200 employ the second.

### 4.3 Nozzle

At high supersonic speed the nozzle performance becomes as important as that of the inlet. The Mach 3 turbojet cycle data in table 1 are for an ideal convergent-divergent nozzle which expands the exhaust gases to ambient pressure. With the nozzle pressure ratio of  $P_8/P_{amb}=51.9$  this requires the divergent area ration  $A_9/A_8$  to be as big as 6.12. If instead of the complex convergent-divergent nozzle a simple convergent nozzle would be used then the net thrust would drop by 34% in this case.

In the following we discuss variable area convergent-divergent nozzles that are suited for fighter aircraft with a design Mach number of about 2. For such applications the reheated low bypass turbofan is the engine type of choice. The nozzle pressure ratio in the high supersonic flight regime is between 15 and 20.

Figure 35 shows the gross thrust ratio between convergent-divergent nozzles of various area ratios  $A_9/A_8$  and a convergent nozzle. If the pressure ratio  $P/P_s$  is lower than 2.5 then the performance of the con/di nozzle is worse than that of a simple convergent nozzle because the flow is over-expanded in the divergent part of the nozzle. However, for the pressure ratios 15 to 20 mentioned above one gets with an area ratio of  $\approx 1.6$  up to 10% gross thrust increase. Since gross thrust at high speed is much bigger than net thrust the benefit translates to  $\sim 15\%$  net thrust advantage over an engine with a convergent nozzle.

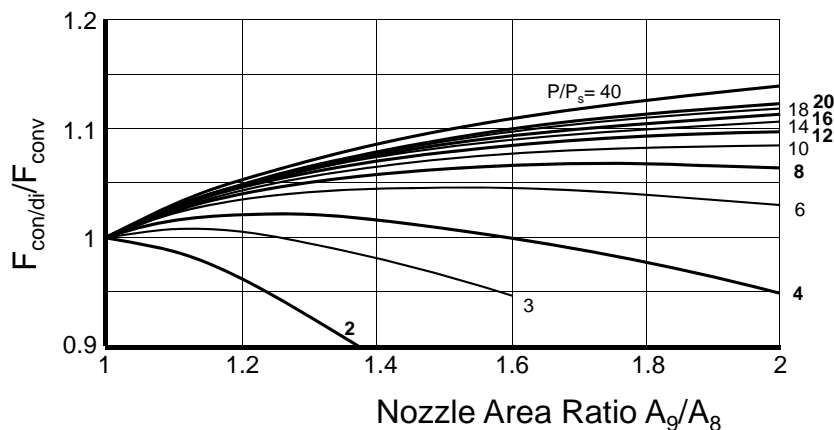


**Figure 35: Thrust Ratio Con Di Versus Con Nozzle.**

Figure 36 shows the flight envelope of a generic augmented fighter engine with lines of constant net thrust difference in % between engines with convergent and convergent-divergent nozzle (area ratio  $A_9/A_8 = 1.6$ ). In the lower left part of the flight envelope the engine with convergent nozzle is superior because the nozzle area ratio is too big for the nozzle pressure ratio under these conditions.

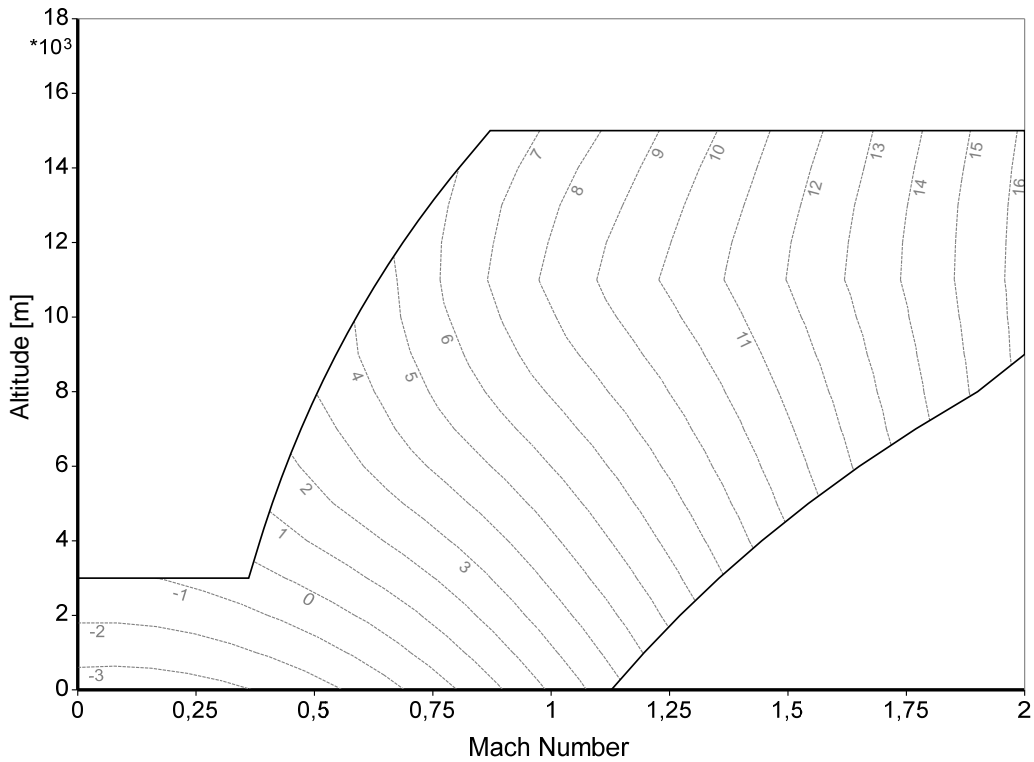
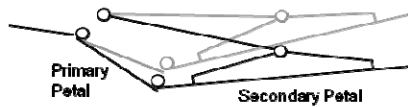


Figure 36: Thrust Gain With a Con/Di Nozzle.

On fighter engines mostly circular convergent-divergent nozzles are used because they are lighter than rectangular nozzles. The basic design of such a nozzle is shown in Figure 37.

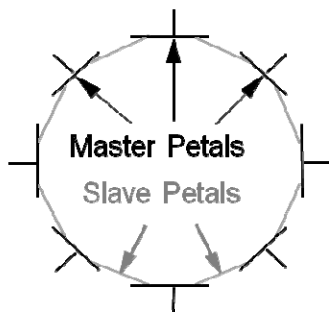
a) Two Positions of the Nozzle



b) Thermal Expansion of the Primary Petals Increases  $A_9/A_8$



c) Rear View



d) Area Ratio =  $f(A_9/A_8)$

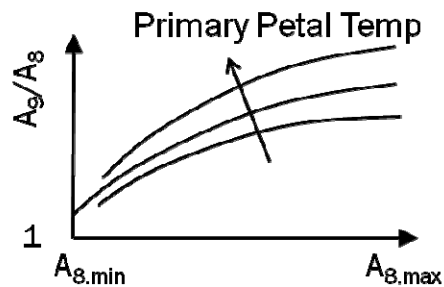


Figure 37: Thrust Ratio Con Di Versus Con Nozzle.

The convergent part of the nozzle consists of the primary petals that are mounted with hinges on the jet pipe. At the end of the primary petals there is another hinge which holds the secondary petals. These petals have a further hinge in the middle of their backside which connects them via a strut to the jet pipe.

The primary petals are opened when the nozzle throat area  $A_8$  needs to be increased, see Fig. 37 a. The secondary petals, held by the primary petals and the strut move in such a way that the nozzle area  $A_9$  increases more than the nozzle throat area  $A_8$  and therefore  $A_9/A_8$  is a function of  $A_8$  (see Fig. 37 d).

Fig. 37c explains why the achievable nozzle area ratio range of a circular con-di nozzle is limited: If the master petals are fully closed then the slave petals will (nearly) touch each other. If they are fully open, then the slave petals will just close the gap between the master petals.

Note that the area ratio does not only change when the nozzle actuator intentionally changes the throat area.  $A_9/A_8$  is also affected by the thermal expansion of the primary petal because the length of the strut which holds the divergent petals remains practically unaffected by the temperature of the gas inside the nozzle (see Fig. 37b). To give an order of magnitude, during dry operation – when the primary petals are relatively cold – the nozzle area ratio is approximately 10 to 15% smaller than with reheat on.

Figures 38 and 39 show the convergent-divergent nozzle of the EJ200. The throat area is varied by moving a ring axially with hydraulic actuators. On the inner side of the moving ring there are rollers which travel on the especially shaped roller track and open or close the primary petals.

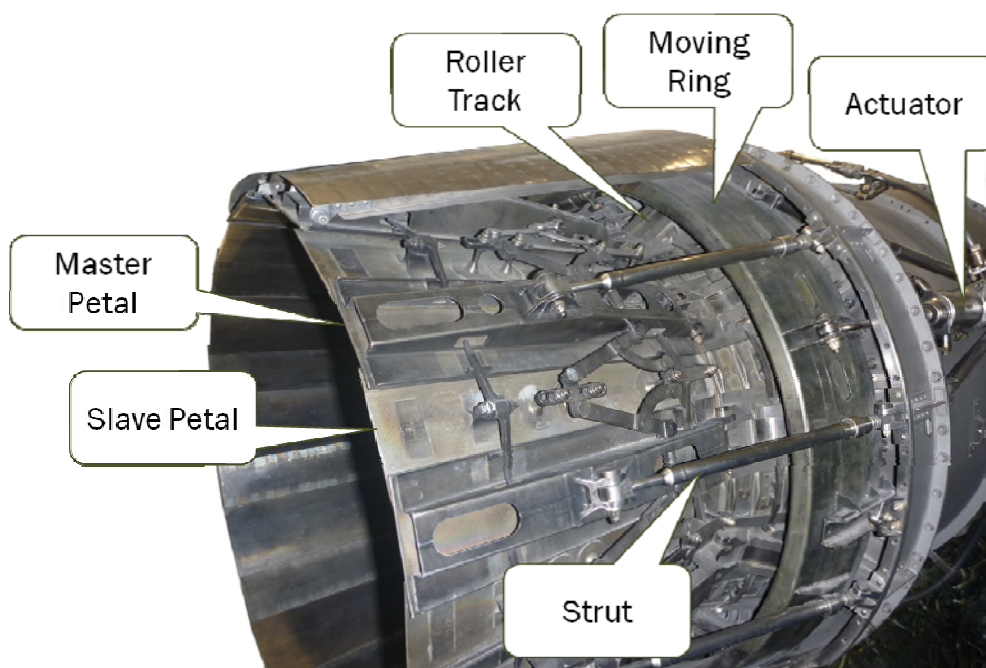


Figure 38: EJ200 Con/Di Nozzle.

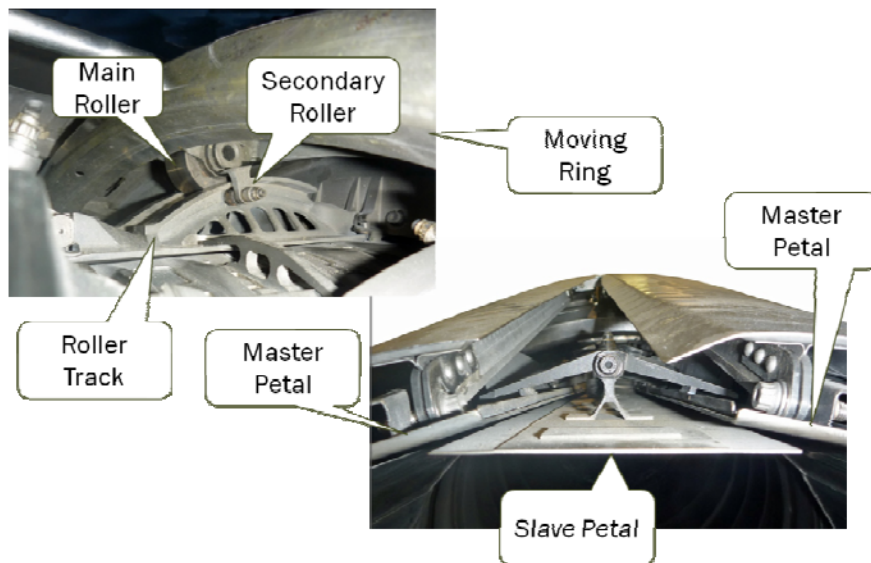


Figure 39: EJ200 Con/Di Nozzle Details.

Note that while in a convergent nozzle the pressure inside the nozzle is always higher than ambient pressure this is not the case with a convergent-divergent nozzle. Think of the flow in a venturi which is a convergent-divergent flow channel with subsonic flow. Even with supersonic flow the pressure inside the nozzle can be lower than ambient pressure - that is the case when the nozzle area ratio is too big and the flow over-expands in the divergent part. Because of these possible flow patterns one needs two devices that prevent the nozzle from collapsing: one is the small roller below the roller track and the other the v-shaped bar that prevents the slave petal from being sucked into the divergent part of the nozzle, see Fig. 39.

During engine development testing of the EJ200, one could easily identify when the pressure inside the divergent nozzle section was lower than outside. The area ratio is bigger than ideal for this pressure ratio and the flow is over-expanded. Inspection of the Figure 40 shows that the slave petals are sucked inwards and a gap opens between the master and the slave petals. This is not a bad thing because the air flowing through the gaps into the divergent part of the nozzle makes the effective nozzle area ratio smaller than the geometric one. The losses due to over-expansion are reduced and thus the nozzle performs better than without the gaps between the petals. The thrust deficit in the lower left part of the flight envelope relative to a convergent nozzle as shown in Fig. 36 is in reality much smaller than derived from theory.

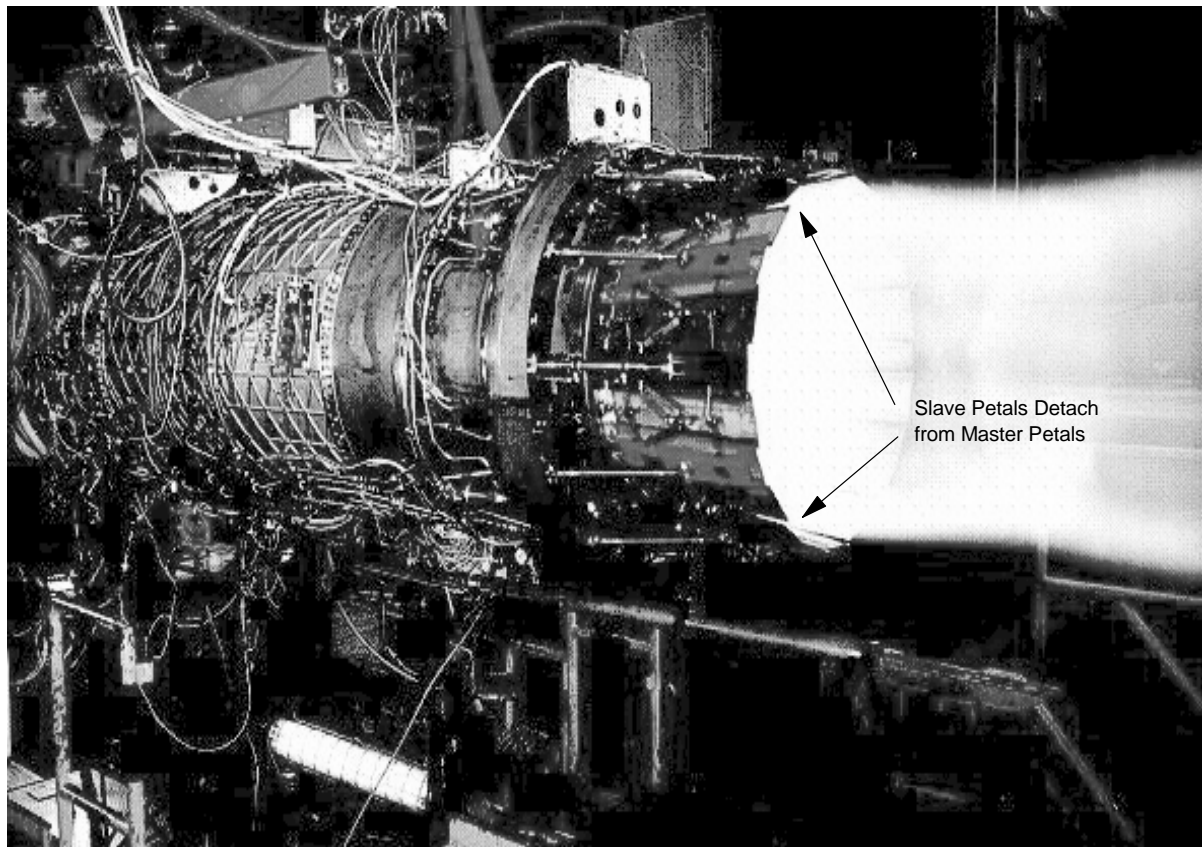


Figure 40: EJ200 at Full Reheat.

## 7.0 REFERENCES

- [1] Louis A. Povinelli: Technical Challenges for Commercial Supersonic Propulsion, ASME GT2010-23720, 2010.
- [2] Peter W. Merlin: Design and Development of the Blackbird: Challenges and Lessons Learned, AIAA 2009-1522, 2009.
- [3] Michel E. Brazier, Randy E. Paulson: Variable Cycle Engine Concept, ISABE 93-7065, 1993.
- [4] J.E. Johnson: Variable Cycle Engine Concepts, AGARD PEP Symposium on “Advanced Aero-Engine Concepts and Controls”, Seattle, USA 1995 and published in CP-572.
- [5] Douglas G. Shafer, Nancy B. McNelis: Development of a Ground Based Mach 4+ Revolutionary Turbine Accelerator Technology Demonstrator (RTATD) for Access to Space, ISABE 2003-1125.
- [6] Jimmy Tai, Bryce Roth, Dimitri Mavris: Development of an NPSS Variable Cycle Engine Model, ISABE 2005-1295.
- [7] Joachim Kurzke, Claus Riegler: A Mixed Flow Turbofan Afterburner Simulation for the Definition of Reheat Fuel Control Laws, RTO AVT Symposium “Design Principles and Methods for Aircraft Gas Turbine Engines” Toulouse, France, 1998 and published in RTO-MP-8, 1999.

- [8] Various Authors: Performance Prediction and Simulation of Gas Turbine Engine Operation, Technical Report RTO-TR-044, published 2002.
- [9] Joachim Kurzke: Gas Turbine Performance Software, [www.gasturb.de](http://www.gasturb.de).
- [10] P.P. Walsh, P. Fletcher: Gas Turbine Performance, 2nd Edition, Co-published by Blackwell Science Ltd. and ASME, 1994.
- [11] H. G. Münzberg: Flugantriebe, Springer Verlag Berlin Heidelberg New York 1972.
- [12] James St. Peter: The History of Aircraft Gas Turbine Engine Development in the United States ... A Tradition of Excellence, International Gas Turbine Institute of ASME, 1999.